МІНІСТЕРСТВО ОСВІТИ ТА НАУКИ УКРАЇНИ

НАЦІОНАЛЬНИЙ ТЕХНІЧНИЙ УНІВЕРСИТЕТ
«ХАРКІВСЬКИЙ ПОЛІТЕХНІЧНИЙ ІНСТИТУТ»

Ministry of Education & Science of Ukraine
National Technical University
«Kharkiv Polytechnic Institute»

РІЗАННЯ ТА ІНСТРУМЕНТИ в технологічних системах

CUTTING & TOOLS IN TECHNOLOGICAL SYSTEM

Міжнародний науково-технічний збірник
International Scientific-Technical Collection

Заснований у 1966 р. М. Ф. Семко
Found by M. F. Semko in 1966

ВИПУСК № 95
Edition № 95

Харків НТУ «ХПІ» – 2021 – Kharkiv NTU «KhPI»

ББК 34.63
УДК 621.91

Державне видання
Свідоцтво Державного комітету телебачення і радіомовлення України
КВ № 7840 від 8 вересня 2003 року
Друкується за рішенням Вченої Ради НТУ "ХПІ",
протокол № 12 від 29 грудня 2021 р.

У збірнику представлені наукові статті, в яких розглядаються актуальні питання в області механічної обробки різних сучасних матеріалів із застосуванням високопродуктивних технологій, нових методик, вимірювальних приладів для контролю якості оброблених поверхонь і високоефективних різальних інструментів. Розглядаються аспекти оптимізації та математичного моделювання на різних етапах технологічного процесу.

Для інженерів і наукових співробітників, що працюють в області технології машинобудування, різання матеріалів, проектування різальних інструментів в технологічних системах.

Науковий збірник «Різання та інструменти в технологічних системах» включений в Перелік фахових видань України категорії «Б», наказ МОН України від 17.03.2020 р., №409

Р34 Резание и инструменты в технологических системах: Междунар. науч.- техн. сб. – Харьков: НТУ «ХПИ», 2021. – Вып. 95. – 80 с.

Адреса редакційної колегії: вул. Кирпичова, 2, Харків, 61002, Національний технічний університет «Харківський політехнічний інститут», кафедра «Інтегровані технології машинобудування» ім. М.Ф. Семка, тел. +38 (057) 706-41-43.

ББК 34.63

UDC 621.9 **doi: 10.20998/2078-7405.2021.95.01**

V. Kovalev, G. Klymenko, Y. Vasylchenko, M. Shapovalov,
O. Antsiferova, I. Maiskykh, Kramatorsk, Ukraine

RESULTS OF INDUSTRIAL TESTING OF CARBIDE CUTTING TOOLS BY PULSED MAGNETIC FIELD TREATMENT AND THE EFFECT ON THE INCREASE OF THE CUTTING PROCESS EFFICIENCY

Abstract. *The task of increasing the efficiency of machining parts on heavy machines was determined, scientifically substantiated and solved by hardening a carbide tool the pulsed magnetic field processing (PMFP). The efficiency of machining of parts is understood as an increase in its productivity, a reduction in the cost and costs of tool materials, and an increase in instrument reliability. The working conditions of cutting tools at heavy engineering enterprises are analyzed. The wear resistance of carbide cutting tools, which have been strengthened by the PMFP, was investigated using forced test methods and modeling of the cutting process. The mechanism of changing the properties of a hard alloy under the action of a pulsed magnetic field is established. The main factors affecting the change in the wear resistance of a hard alloy under the action of a pulsed magnetic field are identified. The effect of pulsed magnetic field processing on the performance of carbide cutting tools under production conditions is investigated. The effect of hardening on productivity, cost of operation and instrumental costs is established. The interrelation of the parameters of the PMFP, the parameters of the process of machining parts and production efficiency is investigated. A statistical model has been developed that allows determining the productivity of mechanical processing depending on the properties of the tool material and the processing parameters of a pulsed magnetic field.*

Keywords: *pulsed magnetic field processing; carbide tools; heavy machine production tests; sustainability; magnetic field strength; pulse frequency; performance.*

Introduction

An important task is to improve the tooling of new machines for high-precision productive machining of difficult-to-machine materials by applying the latest tool strengthening methods. An analysis of different methods for enhancing the physical and mechanical properties of hard-alloy tool materials showed that the best combination of cost and production efficiency was observed with the pulsed magnetic field machining method. In this study, metal machining efficiency was evaluated in terms of objective functions which characterise productivity Q, cost C and tooling cost S depending on tool resistance and cutting modes. In these functions, the influence of tool resistance dissipation was also taken into account. It is established that in hard conditions of cutting it is reasonable to optimize a cutting mode taking into account the dissipation of the tool resistance. As in production conditions the tool resistance dissipation takes place, the cutting conditions should be prescribed in order to ensure the durability with a given reliability P.

This resistance is called gamma percent resistance and is determined with the help of tool failsafe operation graphs, compiled by the results of observations of tool operation. The use of machining by pulse magnetic field of hard-alloy tools increases the value of optimal feed by a factor of 1.2-1.3.

As the industry develops, the demands on machine tools, increasing precision and quality of their manufacture, and the introduction of new, stronger materials that enable higher levels of performance are increasing. An important task is to improve the tooling of new machines for high-precision productive machining of difficult-to-machine materials through the use of the latest tool strengthening methods. One of the perspective technologies for increasing strength, service life and operational properties of metal products for various fields of technology is machining with a pulsed electromagnetic field.

This is particularly relevant for hard-alloy cutting tools. It is well known that hard alloys have, on the one hand, a high heat resistance, which allows cutting tools to operate at high cutting speeds. On the other hand, hard alloys have a low bending strength, which limits their ability to work in previous, roughening operations, where the tool is subjected to shock loads, which are generated by workpieces made by casting or forging methods, abrasive dust, unevenness of assumptions, etc.

Analysis of different methods of improving the physical and mechanical properties of hard-alloy tool materials has shown that the best combination of cost and production efficiency is observed in the method of machining by pulsed magnetic field (MPMF). The essence of MPMF is that the metal-cutting tool before machining is placed in a cavity of a magnet connected to a pulse generator. Under magnetic influence the metal changes its physical and mechanical properties. The magnetic pulse field interacts with the metal-cutting tool material, changing its thermal and electromagnetic properties and improving its structure and performance. Improved properties in metal-cutting tools are achieved by directing the free electrons of the material by an external field, resulting in an increase in the thermal and electrical conductivity of the material. The main advantages of MPMF are: strengthening of metal-cutting tools of any design, simplicity of technological tooling and absence of consumables, environmental friendliness, low cost [1-5].

To implement the MPMF process, a control unit is used to set the workpiece machining modes, i.e. to set certain parameters of the magnetic energy and the duration of its effect.

The process which is connected with metals machining with cutting, by definition of Prof. M. Klushin, is a system of cutting, which consists of elements, which in our case are separate processes. The state of the system is characterized by a selection of values of a number of variables (factors, indicators), and the behavior of the system - a sequence of states in time.

Experimental procedure

The system has the property of relative resistance in the sense that it is maintained only within certain limits of variation of its variables. For our case - previous machining of metals with hard-alloy cutting tools that are reinforced with MPMF, the system is represented in Figure.1 as a relationship of parameters that characterise the machining process and production efficiency from MPMF.

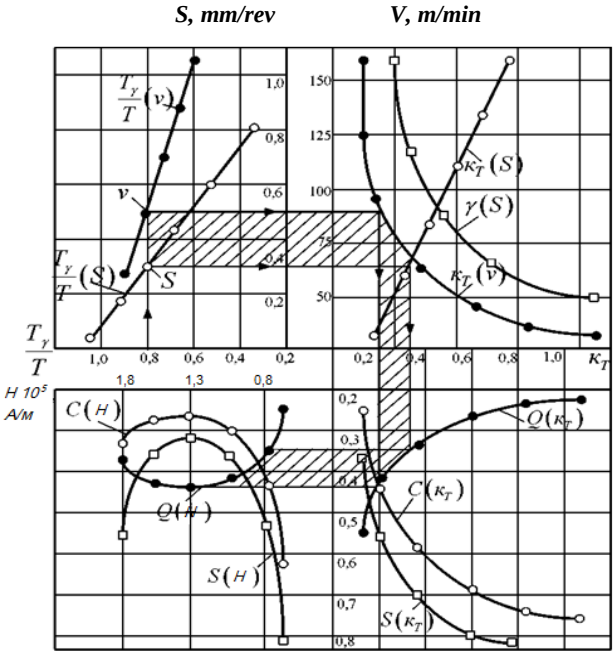

Figure 1 – Relationship between machining parameters and production process efficiency during the use of MPMF

Figure 1 provides recommendations from determining the coefficient of variation of tool resistance KT, Weibull distribution parameter γ, gamma percent tool resistance T_γ depending on given cutting modes ν and S, as well as reasonable values of company efficiency indicators: productivity Q, cost price C and tool costs S. The sequence of connections is defined by arrows.

Due to its autonomy, the mentioned system may be considered as a subsystem or an element of a wider system. The study of the system is carried out by changing external influences on it "at the input" and studying its response "at

the output", which are commonly referred to as functions of the system or parameters of its functioning.

The system state variables in the mentioned case are:

1. The material that is machined, its properties: hardness, strength boundary;
2. The machining operation - removed assumption, reference surface condition, cutting conditions;
3. Cutting tool - tool material (composition, properties), geometric and structural parameters;
4. The stiffness of the system, its dynamic properties;
5. Parameters of the MPMF - strength of magnetic field, frequency of pulses.

The results of system functioning were considered as follows:

1. Resistance of the cutting tool, gamma percent resistance;
2. The variation of resistance;
3. Machining performance;
4. Cost of operation;
5. Tooling costs.

Each of the parameters of system functioning is more or less influenced by all the variables of its state, as well as their mutual influence. In general, the system under consideration is characterized by a large number of possible states and numerous links between its elements, i.e. it is a complex system.

Since at this time the real physical content of the mechanisms through which the interaction of the system's state variables on each of its indicators is carried out remains revealed only in the main features, the relationship between the parameters will be defined in the form of statistical models, which characterize the relationship between the main variable factors of the system and the parameters that characterize the efficiency of production.

Let us present the factors that influence the functioning parameters for such groups:

1 group. Factors that characterize the design and geometric parameters of the tools:

- front angle γ;
- posterior angle α;
- The main angle in the plane φ;

2 group. Factors that characterise the quality of tool construction:

- Rear surface roughness R_{z3n};
- roughness of the front surface R_{z3n};
- Hard alloy hardness boundary $\sigma_в$;

3group. Factors that characterise workpiece quality are:

- unevenness of assumption in the workpiece h_3;

- hardness of the machined material HB;
- strength limit of the machined material σ_B;
- yield strength of the machined material σ_T;

4 group. Factors which characterize the MPMFP process:

- magnetic field strength H;
- pulse frequency f;

5 group. Factors which characterise properties of the tool material:

- HRC hardness;
- durability;
- Red resistance.

The factors given in groups 3 and 5 were not considered because no information could be obtained at the time of screening regarding factors in the production environment that would allow to establish a correlation with tool resistance.

Theoretically, any space can be considered. In practice, this involves more or less time spent on the state of the programme and analysis of the results.

In a first step, a correlation analysis was carried out to screen out the factors beforehand. Behind the dimensions of the correlation characteristics, the density of the correlation between the resistance and the factors can be established and those factors that have the strongest correlation with the tool resistance within its dispersion range can be singled out.

Since there can be both a linear and a non-linear connection between the factors considered and resistance, a correlation relation was used to assess the closeness of this relationship, which was determined using the formula:

$$\eta = \sqrt{\frac{\sigma^2 - \sigma_y^2}{\sigma^2}}, \qquad (1)$$

where $\sigma^2 = \frac{1}{n}\sum(y - \bar{y})^2$, $\sigma_y^2 = \frac{1}{n}\sum(\bar{y}_j - \overline{y})^2$;

$\bar{y}_j$ – group average.

The data for the correlation analysis were obtained under production conditions by testing . Table 1 shows the values of the correlation relations between the resistance and the technological factors, which are calculated according to formula 1.

As can be seen from Table 1, the correlation relationships between resistance and such factors as front angle, main angle in plan, percentage of tungsten carbide has a value from 0.09 to 0.18. This demonstrates that the marked factors have insufficient closeness to the resistance within its dispersion range and, therefore, will not be taken into account further.

Table 1 – Correlation relationships between tool resistance and technology factors

Factors that affect resistance	Correlation ratio
1. Front angle γ	0,18
2. Main angle in plan φ	0,16
3. Percentage of tungsten carbide *WC*	0,09
4. Magnetic field strength *H*	0,48
5. Pulse frequency *f*	0,35
6. Percentage of cobalt C_o	0,42
7. Hard alloy strength limit $\sigma_в$	0,34

The above results of the analysis, although it made it possible to narrow the description space to 7 factors, but did not allow us to identify the dominant factors, so the next stage was to calculate the correlation coefficient between the factors using the expression:

$$r_{ij} = \frac{\sum_{k=1}^{n}(x_{ik}-\overline{x_{ik}})(x_{jk}-\overline{x_{jk}})}{\sqrt{\sum_{k=1}^{n}(x_{ik}+\overline{x_{ik}})^2 \sum_{k=1}^{n}(x_{jk}-\overline{x_{jk}})^2}}, \quad (2)$$

where *i*, *j* – the numbers of the factors between which the inter-correlation coefficient is calculated;
x_{ik}, x_{jk} – pair of factors in question;
$\overline{x_{ik}}$, $\overline{x_{jk}}$ – average values of the factors.

$$\overline{x_{ik}} = \frac{1}{n}\sum_{k=1}^{n} x_{ik}\,, \quad \overline{x_{jk}} = \frac{1}{n}\sum_{k=1}^{n} x_{jk}\ .$$

The significance of correlation coefficients was assessed using Student's criterion :

$$|r| = \frac{t_{кр}}{\sqrt{t_{кр}^2+n-2}}. \quad (3)$$

It should be noted that if the calculated value of the correlation coefficient r turns out to be greater than the assumed value (14), then the mutual influence of the pair of factors xi and xj cannot be neglected.

The statistic which characterises the contribution of any factor to the total variance was the assumed variance of the normalised value of that factor. The factors were normalised by this transformation:

$$x_{ik} = \frac{x_{ik}-\frac{x_{imax}+x_{imin}}{2}}{\frac{x_{imax}-x_{imin}}{2}}, \quad (4)$$

where xi is the current value of the factor in physical terms;
x _ imax, x _ imin - maximum and minimum value of the ith factor.

The marked transformation allows all properties to be reduced to a single scale and provides the opportunity to compare them from each other. The variance of the normalised values was determined by the formula:

$$\sigma\{x_i\}=\frac{\sum_{k=1}^{n}(x_{ik}-\overline{x_{ik}})^2}{n-1} \quad (5)$$

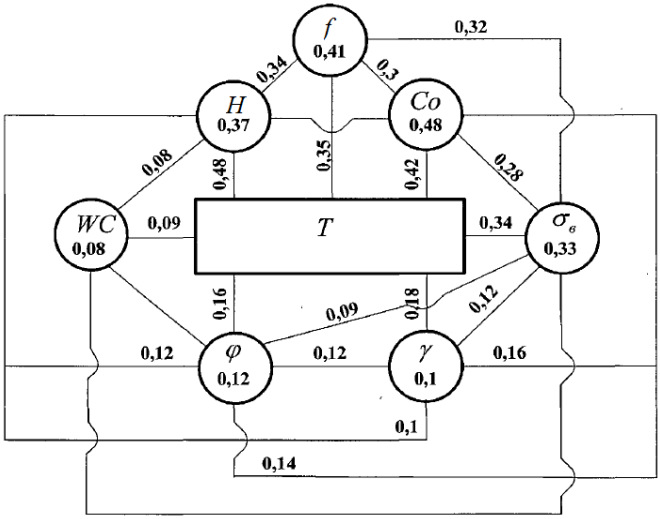

Figure 2 – Diagram of the relationship between factors and the relationship of factors to resistance

Figure 2 shows a diagram of the relationship between the factors and the relationship between the factors and resistance. The sizes of the variances of the normalised values in circles are shown for the main attributes. The lines that connect the attributes correspond to the highlighted relationship. The size of the latter can be judged by means of correlation coefficients, which are shown in the marked scheme.

Thus, the preliminary studies suggest that the dominant factors are the magnetic field strength *H*, the hard alloy strength boundary σv, the cobalt content in the C_o hard alloy, and the pulse frequency f.

As a model to describe the dependence of machining performance, which was defined by formula, on the variation of magnetic field strength x_1 *(H)*, pulse

frequency x_2 *(f)*, cobalt content in the hard alloy x_3 *(C_o)*, hard alloy strength limit x_4 *($\sigma_в$)*, the first degree equation with interactions was applied:

$$y = b_0 + b_1x_1 + b_2x_2 + b_3x_3 + b_4x_4 + b_{12}x_1x_2 + b_{13}x_1x_3 + b_{14}x_1x_4 + b_{23}x_2x_3 + \\ + b_{24}x_2x_4 + b_{34}x_3x_4 + + b_{123}x_1x_2x_3 + b_{234}x_2x_3x_4 + b_{134}x_1x_3x_4 + \\ + b_{124} + x_1x_2x_4 + b_{1234}x_1x_2x_3x_4. \quad (6)$$

The above equation can be obtained by varying each of the factors x_i at the upper x_{iv} and lower xin levels, which differ from the base level xio by the size of the variation step $\pm\Delta x_i$.

A complete factor experiment of the form 2^4 has been adopted as the basis of the experimental plan, where 2 is the number of levels (upper and lower) of independent variables; 4 is the number of independent fungible variables.

This plan allows for all possible unrepeated combinations of levels of independent variables, each of which is forced to vary at two levels.

To simplify the calculations, the independent variables were coded by the transformation formula :

$$z_i = \frac{x_i - x_{i0}}{\Delta x_i} \quad (7)$$

The size of the lower and upper level and, respectively, the size of the variation step for each variable had the following values:

– *H*: $x_{1н} = 0{,}8 \cdot 10^5$ А/м, $x_{1в} = 1{,}3 \cdot 10^5$ А/м , $\Delta x_1 = 0{,}25$;

– *f*: $x_{2н} = 5$ Hz, $x_{2в} = 10$ Hz, $\Delta x_2 = 2{,}5$;

– C_o: $x_{3н} = 6$ %, $x_{3в} = 10\%$; $\Delta x_3 = 2$;

– $\sigma_в$: $x_{4н} = 5{,}1 \cdot 10^8$ Pa, $x_{4в} = 6{,}3 \cdot 10^8$ Pa, $\Delta x_4 = 0{,}6$.

Each row shows the levels of values of the variables that have been assigned to a particular point in the factor space.

The coefficients of the interproximal function were determined by the formula:

$$b_i = \frac{\sum_{m=1}^{N} x_{im} y_m}{N}. \quad (8)$$

Mathematical model of dependence of machining capacity on parameters of change of magnetic field strength x_1 *(H)*, pulse frequency x_2 *(f)*, cobalt content in hard alloy x_3 *(C_o)*, hard alloy strength limit x_4 *($\sigma 4$)* according to results of conducted test can be written in the form:

$$y = 2{,}795 + 0{,}828z_1 + 0{,}025z_2 + 0{,}358z_3 + '0{,}369z_4 - 0{,}006z_5 + \\ + 0{,}115z_6 + 0{,}126z_7 + 0{,}016z_8 + 0{,}027z_9 - 0{,}148z_{10} - 0{,}117z_{11} + \\ + 0{,}145z_{12} - 0{,}102z_{13} - 0{,}019z_{14} - 0{,}049z_{15}. \quad (9)$$

Conclusions

1. It has been established that the use of pulse magnetic field machining improves the optimum resistance by a factor of 1.4-2.

2. For tools, which work in conditions of heavy cutting, use of pulse magnetic field machining promotes increase of optimum feed by a factor of 1,15-1,3 times.

3. Using the factor analysis of 24, type, the dependence of machining productivity of cutters, which are reinforced with MPMF, from intensity of magnetic field H, hard alloy strength limit σv, cobalt content in hard alloy Co, pulse frequency *f* was determined

References: 1. *Quan S.* Effect of pulsed magnetic field treatment on the residual stress of 20Cr2Ni4A steel / Quan S., Jiajie K., Zhiguo X., Haidou W., Yanfei H., Guozheng M., Haipeng L. // Journal of Magnetism and Magnetic Materials. – 15, April 2019. Volume 476. – pp. 218-224. https://doi.org/10.1016/j.jmmm.2018.12.105. **2**. *Huang Xinquan C.* Residual stress reduction by combined treatment of pulsed magnetic field and pulsed current / Huang Xinquan C. // Materials Science and Engineering:A., 25 July 2011. – Volume 528. – Issues 19-20/ – pp. 6287-6292. https://doi.org/10.1016/j.msea.2011.04.078. **3**. *Ma L.* An investigation on the mechanical property changing mechanism of high speed steel by pulsed magnetic treatment / Ma L., Zhao W., Liang Z., Wang X., Xie L., Jiao L., Zhou T. // Materials Science and Engineering: A., 15 July 2014, – Volume 609. – pp. 16–25. https://doi.org/10.1016/j.msea.2014.04.100. **4.** *Shapovalov M. Kovalov V., Vasylchenko Y.* Increase the productivity of hard-alloy tools for heavy machine tools by processing impulse magnetic field *Вісник ТНТУ*. Тернопіль, 2018. № 3 (50). С. 52–59. **5.** *Kovalov V., Vasilchenko Y., Shapovalov M, Turmanidze R., Dašić P.* Impact of a Pulsed Magnetic Field on a Hard Alloy During Machining on Heavy Machine Tools. International Journal of Industrial Engineering and Management (IJIEM), Vol. 10 No 1, 2019, Pp. 125–130. ISSN 2217-2661. https://doi.org/10.24867/IJIEM-2019-1-125. **6.** *Rodichev Y., Soroka O., Kovalov V., Vasilchenko Y., Maiboroda V.* (2020) Fracture Resistance of the Edge of Cemented Carbide Cutting Tool. In: Tonkonogyi V. et al. (eds) Advanced Manufacturing Processes. InterPartner 2019. Lecture Notes in Mechanical Engineering. Springer, Cham. https://doi.org/10.1007/978-3-030-40724-7_29.

Віктор Ковальов, Галина Клименко, Яна Васильченко, Максим Шаповалов, Олеся Анциферова, Ігор Майських, Краматорськ, Україна

РЕЗУЛЬТАТИ ПРОМИСЛОВИХ ВИПРОБУВАНЬ ТВЕРДОСПЛАВНОГО РІЗАЛЬНОГО ІНСТРУМЕНТУ ОБРОБЛЕНОГО ІМПУЛЬСНИМ МАГНІТНИМ ПОЛЕМ І ВПЛИВ НА ПІДВИЩЕННЯ ЕФЕКТИВНОСТІ ПРОЦЕСУ РІЗАННЯ

Анотація. *Поставлено, науково обґрунтовано та вирішено завдання підвищення ефективності обробки деталей на важких верстатах шляхом зміцнення твердосплавного інструменту обробкою імпульсним магнітним полем (ОІМП). Досліджено зносостійкість твердосплавних різальних інструментів, зміцнених ОІМП, з використанням методів форсованих випробувань та моделювання процесу різання. Встановлено механізм зміни властивостей твердого сплаву під впливом імпульсного магнітного поля. Виявлено основні чинники, що впливають на зміну зносостійкості твердого сплаву під впливом імпульсного магнітного поля.*

Досліджено вплив обробки імпульсним магнітним полем на працездатність твердосплавного різального інструменту у виробничих умовах. Встановлено вплив загартування на продуктивність, вартість експлуатації та інструментальні витрати. Проведено оцінку ефективності обробки металів різанням за цільовими функціями, що характеризують продуктивність Q, собівартість C і інструментальні витрати S в залежності від стійкості інструментів і режимів різання. У цих функціях враховувалося також вплив розсіювання стійкості інструментів. Оцінка ефективності обробки металів різанням дозволила встановити підвищення оптимальної стійкості інструментів, зміцнених ОІМП в 1,4–2,5 рази, а також дати практичні рекомендації щодо визначення оптимальної подачі. Використовуючи результати виробничих випробувань, на основі принципів системного підходу представлено взаємозв'язок параметрів механічної обробки і ефективності виробничого процесу при використанні ОІМП. Розроблено статистичну модель, що дозволяє визначити продуктивність механічної обробки залежно від властивостей інструментального матеріалу та параметрів обробки імпульсним магнітним полем. Після оцінки кореляційних відношень за допомогою повного факторного експерименту була визначена залежність продуктивності обробки зміцненими різцями від домінуючих чинників: напруженості магнітного поля, межі міцності твердого сплаву, вмісту кобальту в твердому сплаві, частоти імпульсів, яка має практичне застосування.

Ключові слова: *оброблення імпульсним магнітним полем; твердосплавний інструмент; важкий верстат; виробничі випробування; стійкість; напруженість магнітного поля; частота імпульсів; продуктивність.*

UDC 004.94(045) **doi: 10.20998/2078-7405.2021.95.02**

H. Matyi, P. Tamás, Miskolc, Hungary

DIGITAL TWIN TECHNOLOGY IN LOGISTICS LITERATURE REVIEW

Abstract. *The digital twin has been released in a number of industries that include logistics as well, with the creation of new research areas. To find the research area, a complex literature analysis is required. At present, publications in scientific journals and publications on the Internet are more important than print-based literature. Because of this, you can get huge results with a single search. It is important that you can analyze these databases well. One method of this analysis is systematic literature review.*
Keywords: *digital twin; logistics; systematic literature review.*

INTRODUCTION

Today, we are living in a digital revolution. In this way, digitalisation has transformed jobs, skills and the relationship between employer and employee. Most people live in a digital environment, so it's important to make full advantage of it. Digital transformations have many benefits, even in longer term. One of the most significant inventions of the 4th Industrial Revolution was the digital twin. This technology will be presented in the publication, such as its concept, version, and options for its application.

We analyze the research of the digital twin so far with a systematic literature review. This method is essential for analyzing published article's results. To analyze the success of the topic area, we create an annual chart of the publications published. For this, we define several keyword search methods as well as a combined search. The results are summarized to illustrate the results.

The purpose of the publication is to analyze them after a literature review. Highlighting the digital twin application in the field of logistics.

MEAN FEATURES OF DIGITAL TWIN

The digital twin is a virtual version of an object or system that spans its lifecycle, contains real-time data and uses simulation, machine learning. With digital twin the decision making is easier. The digital twin is the creation of a complex virtual model that is the twin sibling of a physical object. The digital twin is a vital tool for understanding not only the performance of the current product but also its future state [1].

The implementation of digital twin technology is possible with the Internet of Things as well as data analysis. As a first step, they create a mathematical model

that properly simulates the original. Secondly, it has to be sure that the virtual model recieves feedback from the sensors that collect data from the real version. This allows the digital twin to show what happened to the original version in real time. The digital twin can be used in conjunction with a prototype to provide feedback on the product during development [5].

There are two versions of the digital twin. A digital twin prototype, which contains information that can be used to describe a real product. These can be the manufacturing process, 3D modell, bill of materials. The other version is the digital twin instance, which is a virtual product linked to a physically existing product. It contains the geometric data of the real object, 3D model, parts list, maintance results and information [2].

The application of the digital twin depends on which stage of the product lifecycle it models. They can be used in three main parts. These are product development, manufacturing and product design and the third one is the performance increasing. Using a digital twin, you can effectively design a new product. The twin allows you to virtually check the performance of the product, making visible how it affects the physical word. In this case, a virtual-physical connection is created that allows you to analyze how a product performs under different conditions. This reduces the need for multiplie prototypes. The use of digital twins can be analyzed by manufacturing and product design before production begin. If more digital twins are created from all production facilities, production can be further optimized. The digital twin created to increase performance generates a huge amount of data, analyzing this data from operating plants, help decision making [17].

METHODS OF LITERATURE REVIEW

Nowadays, publications in scientific journals and publications on the Internet are gaining prominence. Because of this, with one single research could give a huge amount of results. The disadvantage of this is you may encounter inconsistencies and information that may make the content unusable[10].

The systematic literature review is a high level, comprehensive study of a scientific methodology that summarizes and analyzes all the existing research findings on a given problem [6].

A systematic review of the scientific literature in a given field is improtant to indentify research questions and to justify future research in that field. This is a compley process, so it is important to know the right databases to conduct research [3].

APPLIED METHODOLOGY

We did the literature review using Systematic Literature Review (SLR) method. In practice, the usefulness of a research is mainly determined by its

prevalence, not its print appearance. The SLR contains documentation of all methods performed [8].

Traditionally, literature reviews present research results in descriptive or narrative form. A good narrative presentation provides the reader with a comprehensive presentation of the various views of a discipline, including its key methodolodies and theoretical traditions. Denyer and Neely (2004) stated that reports about systematic reviews should include a section on the methodology used and provide an accurate description of the course study. In their view, this mainly necessary so that all decisions are taken in a transparent manner [4].

The aim of our work is to make a transparent scientific presentation of the topic, minimizing bias, through an extensive search for published studies, mainly in English and Hungarian. The goal of the publication is to create a reliable knowledge base.

SLR alone is already a scientific research, although it does not require a laboratory experiment, but involves preliminary design and application of the method [8].

Systematic literature review consists of the following steps: [10], [15]

1. Defining research questions (Who has done something so far? Who did the research or published it first?
2. Discover related literature, primarly using online databases.
3. Reduce results, select relevant publications and determine the main research direction by reading them (determining extra keywords, based on authors, date, etc)
4. Development of a method for processing and analyzing publications.
5. Formulation of major scientific breakthroughs and results.
6. Identifying a scientific gap or bottleneck.

Based on these steps, the following sections can be determined. First, we identify keywords related to digital twin technology. Then, we select databases in which publications can be searched in this regard. We will then gather the information for the relevant articles. [13].

The purpose of this publication is to present the research topic and literature sources using the Scopus, Web of Science and ScienceDirect databases.

DATABASES

We did our research in 3 databases. On Scopus, Web of Science and ScienceDirect. The keywords we searched for were the same in all three databases. When analyzing the literature, the first keywords were the followings, and their most important combinations:

- „artificial intelligent”
- „digital twin”
- „digital twin technology”

- „logistics”
- „packaging”
- „transportation”

The search was conducted primarly with the words artificial intelligence, digital twin and digital twin technology. We first performed each field and then set a filtration search to title, abstract, and keywords. It is important to note that the analyzes were performed on 18th of November, 2021., since then more publications may have appeared. The time interval was narrowed from 2000 to 2021.

Table 1 summarizes the datas.

It is clear from the table that there is a growing number of publications in the subject area. It can be observed that most of the publications are in the Scopus database, then in the ScienceDirect and finally in the Web of Science database.

Subsequently, we also performed a combination search in the Scopus and then in the ScienceDirect database. The combined search in the Scopus database did not get any results. The combination keywords are:

- „digital twin” AND „logistics” OR „digital twin technology” AND „logistics”
- „digital twin” AND „logistics” AND „packaging” OR „digital twin technology” AND „logistics” AND „packaging”
- „digital twin” AND „logistics” AND „transportation” OR „digital twin technology” AND „logistics” AND „transportation”

Than, we did a combine and filter research. The results is shown in a chart of the number of publications published per year.

The first search combination „digital twin” AND „logistics” OR „digital twin technology” AND „logistics” we got 855 publication results at the end of 2021. Its annual analysis is shown in the following figure.

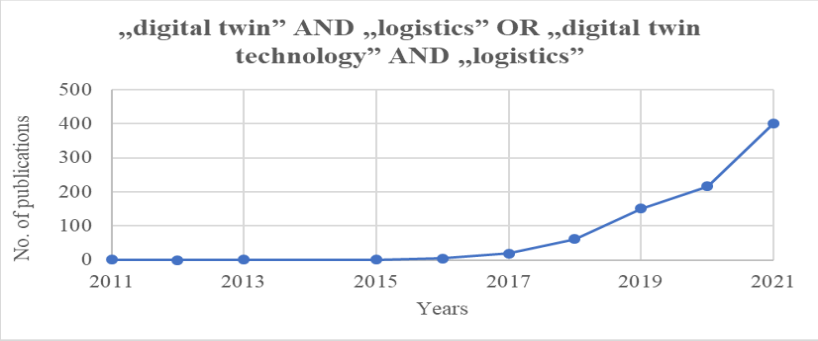

Figure 1 – ScienceDirect combined search results 1. (own editing)

Table 1 – Searched datas (own editing)

	Search fields	Searched key words	2000-2021	2000	2001	2002	2003	2004	2005	2006	2007	2008	2009	2010	2011	2012	2013	2014	2015	2016	2017	2018	2019	2020	2021
Scopus	all field	"Artificial Intelligent"	9577	52	68	93	94	160	181	201	204	222	276	351	396	381	408	357	438	528	525	722	1101	1361	1458
	title, abstract, key words		3364	23	28	28	41	64	74	82	88	119	139	142	138	139	118	139	149	185	277	439	463	411
	all field	"Digital Twin"	11731	0	0	0	0	2	5	0	0	0	1	1	3	17	14	13	22	53	184	648	1762	3550	5456
	title, abstract, key words		5384	0	0	0	0	2	4	0	0	0	0	1	1	1	7	2	7	24	120	353	1027	1743	2083
	all field	"Digital Twin Technology"	998	0	0	0	0	0	0	0	0	0	0	0	0	0	0	0	0	0	3	33	127	329	506
	title, abstract, key words		348	0	0	0	0	0	0	0	0	0	0	0	0	0	0	0	0	0	1	13	37	119	178
Web of Science	all field	"Artificial Intelligent"	1398	6	18	13	19	23	22	62	17	33	33	38	36	32	41	33	70	81	66	106	175	257	271
	title, abstract, key words		194	2	2	0	3	3	4	2	3	5	9	8	8	2	9	9	8	10	11	19	21	31	32
	all field	"Digital Twin"	1642	0	0	0	1	1	0	0	0	0	0	0	0	0	0	1	1	1	23	62	193	495	865
	title, abstract, key words		680	0	0	0	0	0	0	0	0	0	0	0	0	0	0	1	1	0	8	21	84	205	360
	all field	"Digital Twin Technology"	101	0	0	0	0	0	0	0	0	0	0	0	0	0	0	0	0	0	0	4	6	36	55
	title, abstract, key words		19	0	0	0	0	0	0	0	0	0	0	0	0	0	0	0	0	0	0	1	2	8	8
ScienceDirect	all field	"Artificial Intelligent"	4129	34	36	54	58	38	54	62	84	89	125	103	138	168	167	154	230	237	283	318	433	552	712
	title, abstract, key words		480	2	9	9	6	2	5	6	6	11	15	11	15	23	16	21	25	17	26	23	53	76	109
	all field	"Digital Twin"	3186	1	3	1	1	0	0	0	0	2	0	3	2	0	4	3	2	20	65	183	486	887	1524
	title, abstract, key words		948	0	0	0	1	0	0	0	0	0	0	0	0	0	0	0	1	2	20	48	157	272	447
	all field	"Digital Twin Technology"	280	0	0	0	0	0	0	0	0	0	0	0	0	0	0	0	0	1	7	28	75	168	
	title, abstract, key words		58	0	0	0	0	0	0	0	0	0	0	0	0	0	0	0	0	0	1	4	20	33	

On Figure 1. an increase can be seen in the numbers of publication. The second search combination is „digital twin" AND „logistics" AND „packaging" OR „digital twin technology" AND „logistics" AND „packaging". The word „packaging" related to my research topic was also included. There are 270 results for this. The results of the annual analysis are shown in Figure 2.

Another area of my research topic is transportation and the digital twin. So, we did the next combined search with these words „digital twin" AND „logistics" AND „transportation" OR „digital twin technology" AND „logistics" AND „transportation". This search combination resulted in 389 publications by 2021. The results are shown in Figure 3.

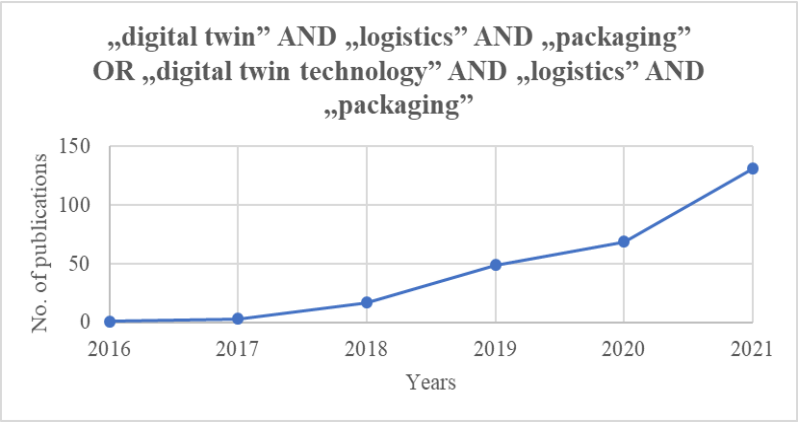

Figure 2 – ScienceDirect combined searched results 2. (own editing)

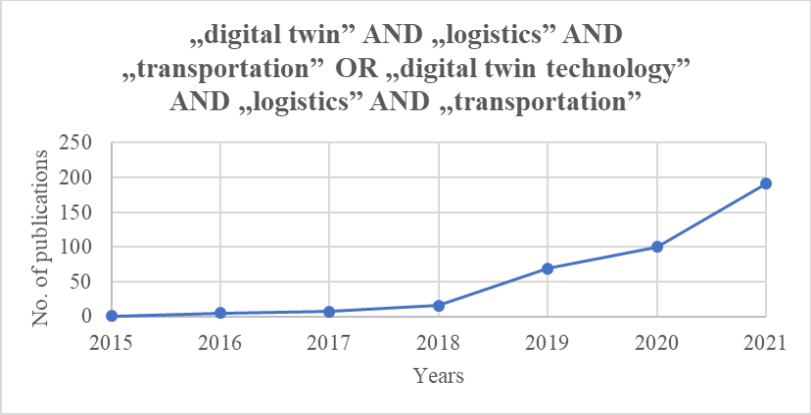

Figure 3 – ScienceDirect combined search results 3. (own editing)

DIGITAL TWIN TECHNOLOGY IN THE LOGISTICS LITERATURE

Digital twin technology has already appeared in many industries. With artificial intelligence and digital twin technology, an intellignt model can be created throughout the supply chain. Using virtual reality creates a better option that helps with various tasks such as vehicle loading [9], [12].

The operation and optimization of complex production and logistics enterprises is driven by actual data and simulation, and therefore requires a multi-

faceted decision-making approach. Digital enterprise systems are complex, so the optimal solution may vary depending on the current situation. In decision making, the digital twin concept can be properly applied, covering the entire lifecycle of a device or process by forming a closed chain [11].

One of the main challenges in digital twin technology is making real-time decisions. The object must be constantly tracked and monitored. The Internet of Things also helps to make real-time decisions in logistics network by calculating, analyzing and optimizing real-time data. [7].

In our opinion, there is a huge potential for the application of digital twin technology in logistics. In our view, the two most important areas will be packaing development as well as transportation development.

DIGITAL TWIN TECHNOLOGY TO IMPROVE PACKAGING

Product and packaging data helps companies increase efficiency, such as optimizing packaging selection and container loading. Expensive and fraigle products, such as pharmaceuticals and electronic components are shipped with sensors that monitor the temperature, the spatial orientation of the packaging, shock and vibration. The latest version of this type of equipment includes sensors that continuously transmit data during cargo transportation [16].

One-used packaging has long been a threat to the environment, especially food packaging. By using the digital twin, errors can be easily filtered out by designing and then testing the packaging in digital space. Today, more and more companies are using biodegradable or reusable packaging. The digital twin can be used to monitor reusable container fleets and their damage [14].

DIGITAL TWIN TECHNOLOGY TO IMPROVE TRANSPORTATION

Reusable containers are the standards for the logistics industry. These include reusable crates between standard ocean-going conatiners, aircraft, auto parts factories and containers for food and beverages to retail stores and end users. It is difficult to track such containers. Companies must not only control the movement of containers, but also check for the presence of any damage or contamination that could endanger future shipments. Using digital twin, collecting and analyzing all the data helps the decisions maker make the optimal decision. It also identifies problems such as rough handling of the container and lack of it. The next step in developing transportation by the digital twin is to include the contents of a package or container in the digital twin. The digital twin pair of the shipment will act as a repository for the data collected by sensors. [16].

SUMMARY

The article introduces the concept of the digital twin, digital technology, and the history of the development of technology.

During a review of the history of literature, articles on the publications published so far, with the search words artificial intelligent, digital twin and digital twin technology were summarized.

The digital twin has already achieved huge success in many areas, but has not yet reached its full potential in logistics. In this publication, we have presented the application of the digital twin in logistics.

ACKNOWLEDGEMENT

"The research work described in this article is the NTP-SZKOLL-20-0022 identifier "Focus'21-Focus on community by developing digital competencies" project, supported by the Ministry of Human Resources and Human Resources Support Manager."

References: **1.** *Armstrong M.M.:* Cheat sheet: What is Digital Twin? (2020), https://www.ibm.com/blogs/internet-of-things/iot-cheat-sheet-digital-twin/ (Last opened: 2021.11.22.). **2.** *Bányai T., Bányainé Tóth Á., Illés B., Tamás P.* (Hungarian book): Ipar 4.0 és logisztika, Miskolci Egyetem, Miskolc-Egyetemváros, ISBN 9789633581827, 2019. **3.** *Torres-Carrión és társai:* Methodology for systematic literature review applied to engineering and education (2018), 2018 IEEE Global Engineering Education Conference (EDUCON), https://doi.org/10.1109/EDUCON.2018.8363388. **4.** *Denyer, D., & Neely, A.* (2004). Introduction to special issue: Innovation and productivity performance in the UK. International Journal of Management Reviews, 5-6(3-4), 131–135.doi:10.1111/j.1460-8545.2004.00100.x **5.** What is Digital Twin Technology and how does it work? https://www.twi-global.com/technical-knowledge/faqs/what-is-digital-twin#HowDoesDigitalTwinTechnologyWork (Last opened: 2021.11.22.). **6.** *Walsh D., Downe S.* (2005) Meta-synthesis method for qualitative research: a literature review, National Library of Medicine https://doi.org/10.1111/j.1365-2648.2005.03380.x. **7.** *Greif T., Stein N., Flath. M. C.,* (2020): Peeking into the void: Digital twins for construction site logistics. **8.** *Ginieis M., Sánchez-Rebull M.-V., Campa-Planas F.* (2011): The academic journal literature on air transport: Analysis using systematic literature review methodology, https://doi.org/10.1016/j.jairtraman.2011.12.005**. 9.** *Jörn Petereit,* Digital twins and Artificial Intelligence in logistics, https://www.cloudflight.io/expert-views/digital-twins-and-artificial-intelligence-in-logistics-44867/ (Last opened: 2021. 11. 22.). **10.** *Kamarási V.; Mogyorósy G.* (2015): Szisztematikus irodalmi áttekintések módszertana és jelentősége. Segítség a diagnosztikus és terápiás döntésekhez, Orvosi Hetilap 156 (38), pp. 1523-1531. **11.** *Kuehn W.,* (2018)(Hungarian publication), Digital twins for decision making in complex production and logistic enterprises, http://doi.org/10.2495/DNE-V13-N3-260-271**. 12.** *Mobinius Editor* (2020). Digital Twins Technology in Logistics 2021: In-Depth Guide, https://www.mobinius.com/blogs/digital-twin-technology-in-logistics (Last opened: 2021. 11. 22.). **13.** *Moustaghfir K.* (2008): The dynamics of knowledge assets and their link with firm performance, Measuring Business Excellent, ISSN: 1368-3047. **14.** 5 Ways Digital Twinning will revolutionize Logistics, https://lot.dhl.com/5-ways-digital-twinning-will-revolutionize-logistics/ (Last opened: 2021. 11. 22.). **15.** *Szentesi Sz.* (2021) Ellátási láncok optimális kialakításának lehetőségei bizományosan értékesítő étrendkiegészítőket gyártó vállalatnál, Phd értekezés (Hungarian publication). **16.** *Schislyaeva, Rostislavovna E., Kovalenko, Alexandrovich E.,* (2021), Academy of Strategic Management Journal, suppl. Special Issue 2., Arden vol.20. (1-17), e-

ISSN: 19396104. **17.** Siemens: Digital Twin, https://www.plm.automation.siemens.com/global/en/our-story/glossary/digital-twin/24465 (Last opened: 2021.11.22.).

Генрієтт Матій, Петер Тамаш, Мішкольц, Угорщина

ТЕХНОЛОГІЯ «DIGITAL TWIN» (ЦИФРОВОГО ПРОТОТИПУ) У ЛОГІСТИЦІ В ЛІТЕРАТУРНОМУ ОГЛЯДІ

Анотація. *Цифровий двійник був випущений у низці галузей, включаючи логістику, зі створенням нових галузей досліджень. Для визначення галузі дослідження необхідно провести комплексний аналіз літератури. Більшість людей живуть у цифровому середовищі, тому важливо повною мірою використати його переваги. Цифрові перетворення мають багато переваг навіть у довгостроковій перспективі. Одним із найзначніших винаходів 4-ї промислової революції став цифровий двійник. Ця технологія буде представлена в публікації, включаючи її концепцію, версію та варіанти її застосування. Ми аналізуємо дослідження цифрового двійника зараз із системним оглядом літератури. Цей метод є важливим для аналізу результатів опублікованої статті. Щоб проаналізувати успішність тематичної галузі, ми складаємо річний графік опублікованих публікацій. І тому ми визначаємо кілька методів пошуку за ключовими словами, і навіть комбінований пошук. Мета нашої роботи - зробити прозору наукову презентацію теми, мінімізуючи упередженість, за допомогою широкого пошуку опублікованих досліджень, переважно англійською мовою. Мета публікації – створити надійну базу знань. Ми провели дослідження у трьох базах даних. У Scopus, Web of Science та ScienceDirect. Ключові слова, які ми шукали, були однаковими у всіх трьох базах даних. Пошук проводився в основному за словами штучний інтелект, цифровий двійник та технологія цифрового двійника. Робота та оптимізація складних виробничих та логістичних підприємств визначається фактичними даними та моделюванням і, отже, потребує багатогранного підходу до прийняття рішень. Цифрові корпоративні системи складні, тому оптимальне рішення може змінюватись в залежності від поточної ситуації. При прийнятті рішень концепція цифрового двійника може бути належним чином застосована, охоплюючи весь життєвий цикл пристрою або процесу утворюючи замкнутий ланцюжок. На наш погляд існує величезний потенціал для застосування технології цифрових двійників у логістиці. На наш погляд, двома найважливішими напрямками будуть розвиток упаковки та розвиток транспорту.*

Ключові слова: *цифровий двійник; логістика; системний огляд літератури.*

UDC 004.94(045) **doi: 10.20998/2078-7405.2021.95.03**

Z. Molnár, P. Tamás, B. Illés, Miskolc, Hungary

USING THE SLP METHOD IN THE DESIGN OF FLEXIBLE MANUFACTURING CELLS

Abstract. *Flexible manufacturing systems are becoming increasingly important as customers increasingly want customized products. Also, the trend of the product life cycles to become shorter and shorter causes the proliferation of flexible manufacturing systems. Proper layout is key to making the manufacturing system truly flexible. Novel research and this article show how the Systematic Layout Planning method can be applied to the design of flexible manufacturing systems and, going further, how the design process can be supported by manufacturing process simulation.*
Keywords: *systematic layout planning; simulation; flexible manufacturing systems.*

1. INTRODUCTION

The essence of flexible manufacturing is adaptability - that is, the ability to adapt to changes in product requirements without compromising quality. The Flexible Manufacturing System (FMS) is the manufacturing method that helps to achieve this and can reduce the production time and the number of resources required.

Flexible production systems need to be designed to adapt to changes, such as small (or significant) changes in a product, the addition of production volumes or completely new products. This, of course, requires automation of key manufacturing processes in these systems, including machining and assembly, loading and unloading, and data processing. Because the system is automated, it relies less on human power than traditional manufacturing methods. The Flexible Manufacturing System consists of two to ten machines, including processing workstations and parts management capability [1], [2].

In the case of flexible production systems, it is very important to minimize losses as even the smallest loss per piece becomes a significant loss due to the large number of pieces. The seven main losses in lean are excess activity, handling, inventory, transportation, waiting, overproduction, and scrap. Four of these losses are due to improper layout design; they are inventory, shipping, waiting, and overcapacity as these are directly related to layout design.

2. SYSTEMATIC LAYOUT PLANNING FROM FMS VIEWPOINT

One of the most common and accepted methods of layout planning is Systematic Layout Planning (SLP), developed by Richard Muter in the 1960s.

Systematic Layout Planning is a comprehensive layout planning method that can be used to plan the layout of entire factories, taking into account the material transport and material supply and also the parameters of each machine group [3]. Systematic Layout Planning is mainly used for large projects. It divides layout design into four main parts and defines activity points that determine how material flows in a production area in manufacturing. Depending on the level and depth of the design, an activity point can be a department (e.g. a machining plant) or even a machine (e.g. a CNC milling machine).

For layout planning of smaller projects, such as the layout of a specific department or even a group of machines, Systematic Layout Planning has a simplified version called Simplified Systematic Layout Planning [4]. This methodology can work well for smaller projects where the material flow is less dominant, but the placement of individual devices and equipment is more important. These can be offices, laboratories, tool storage, maintenance plants, but also flexible production systems.

The method is based on three things that define each layout:

- the relationships between each item
- the space requirement, ie how much space is needed for a given department or machine
- the exact location of the machines of each department, ie where the equipment and machines will be located within the given space on the final layout.

Both Systematic Layout Planning and its simplified version work with 5 basic parameters:

- the product,
- the quantity,
- the process,
- the supporting services and
- the timing.

For simplified layout design, we have 6 steps:

1. charting the relationships
2. establish space requirements
3. diagram activity relationships
4. draw space relationship layouts
5. evaluate the alternative arrangements
6. detail the selected layout plan.

In the first step, we create the connection graph, which is a graph that determines the importance of the connections between each piece of equipment. The importance can be divided into six categories, from what must be next to each other, all the way to the distance between machines is unimportant (Figure 1).

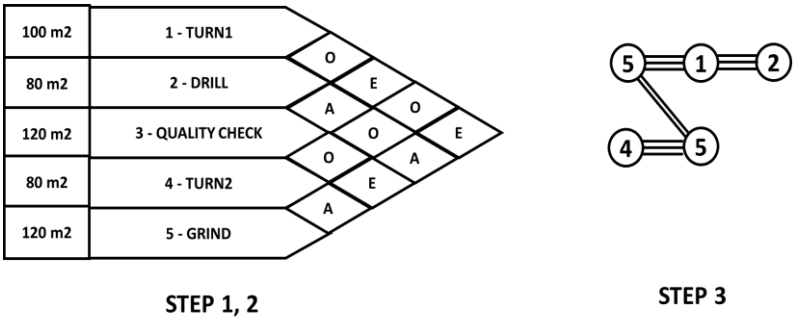

Figure 1 – The first three steps of the Simplified Systematic Layout Planning

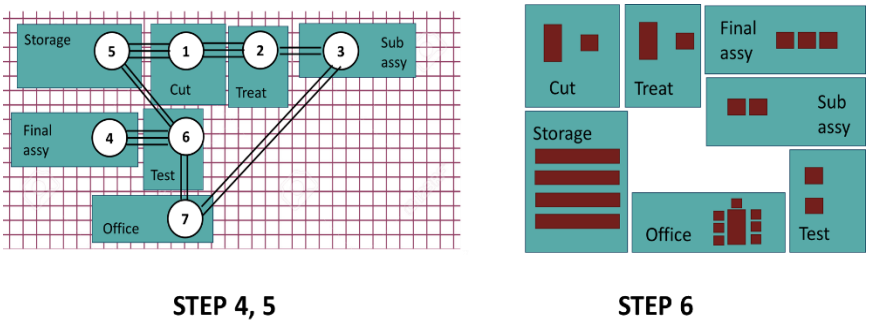

Figure 2 – The last three steps of the Simplified Systematic Layout Planning

In addition, the graph can also be used to indicate the reason why we decided to classify the distances of the two machines and equipment into the given category. Such reasons can be, for example, material flow, maintenance or quite simply a practical reason why it is worth keeping two devices close to each other.

The second step is to specify the space requirements for specific departments or specific equipment. The calculation of space requirements shall consider not only the space directly required by the machinery but also the space requirements around it which belong to the same category or to the same machinery. For example, if a container or a buffer is required for a given machine, the space requirement for that machine must also be included in the machine's space requirement. Separate storage areas should be included in the graph as separate units (Figure 1).

The next step is to draw a graph of activity relationships that shows how important the relationship is between each machine. This can be represented in a graph where the required proximity is typically represented by one, two or three connecting lines (Figure 1).

We can supplement the graph made here with the need for space, as we can draw the size of the required space for each activity point. Regarding the size of the space required, it is worth examining the extent to which it's possible to deviate from the size of the space requirement on the one hand and its proportions on the other. In some cases, an elongated shape is required, whereas, in other cases the proportions of the rectangle determining the space requirement can be changed (Figure 2).

As a result, multiple layout variations can be created that need to be evaluated. Evaluation considerations go beyond simple layout design and may consider parameters that include economics or other practical considerations. Such parameters may include the logistics of the material supply, adaptability within the existing structure, costs, constraints due to the characteristics of the building, and, for example, maintainability or cleanability (Figure 2).

Based on these, the final so-called block layout can be selected, which must be detailed in the last step. During the detailing, the machines and the parameters, storage devices and other objects that are important for the given activity point and that determine its operation, must be drawn (Figure 2).

In the case of flexible manufacturing systems, it is important to highlight that of the five basic parameters, product, quantity, and routing can change quite often. It is also important to see that the life cycle of flexible manufacturing systems can be extended, in most cases with the introduction of a new product, which means that the system must be prepared for the introduction of new elements and new machines during its life cycle.

3. SAMPLE APPLICATION OF THE METHOD

Apparently, this framework provides an easy-to-use and easy-to-understand method for designing production layouts and, as such, can be used for flexible production systems [5], [6].

Figure 3 shows an example of a simple flexible manufacturing system that examines the use of Systematic Layout Planning in a simulation environment. Digital manufacturing support was used for the Plant Simulation discrete event-based simulation system.

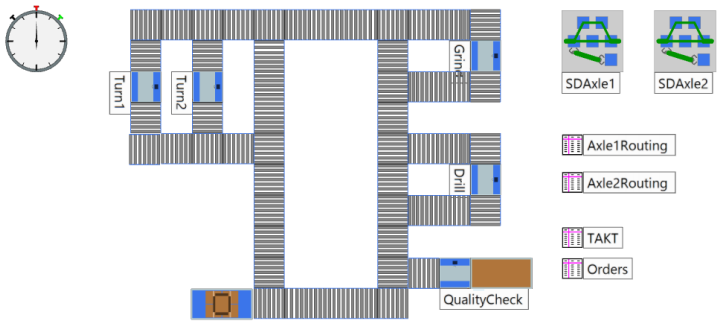

Figure 3 – Simple flexible manufacturing cell layout in simulation environment

The arrangement shown in the diagram produces two products. The technological parameters of the two products are different, the production times are different on each machine and the routing of the two products is also different.

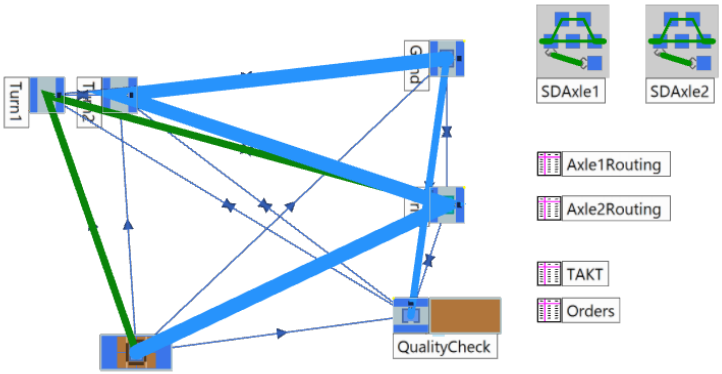

Figure 4 – Material flow by product between the activity points

In the first step, the machining machines are included in the simulation and the parameters that determine the material flow between them. After examining the material flow, it is clear which machine has the strongest material flow, so it is worth placing them as close as possible to each other (Figure 4).

In the next step, different layout variations can be created that can increasingly approach the solution that may work best in terms of space utilization

and technological feasibility. Once the location of the machines has been determined, we must also ensure that the material flows between them, so that the equipment needed for the material flow can operate. A minimum distance must also be defined between the production stations of the various machines and stations.

There are various possibilities for realizing the flow of material between the machines, such as the conveyor track but also the AGVs (Figure 5) [7], [8].

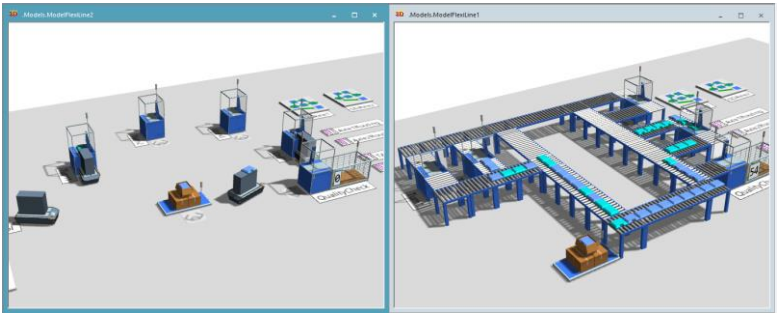

Figure 5 – The first three steps of the Simplified Systematic Layout Planning

Not only do the technological parameters play an important role in the final selection but also, for example, the size of the investment costs, so in the end we decided on the conveyor solution. The final layout ensures that the production system is flexible and complies with the Systematic Layout Planning methodology.

4. SUMMARY

In this article, we examined how a layout design methodology can be used to design increasingly flexible manufacturing systems today. Scaling down the methodologies used to design larger layouts provides a useful solution. Also, during layout design, the steps were well defined and can be mapped well in a discrete simulation environment. The model, which was created in the simulation environment, made it very easy to understand and interpret the layout design parameters and results.

The combination of the systematic layout planning methodology with discrete event-driven simulation, enabled efficient and highly productive layout design. Further steps in the research are aimed at automating the design methodology to the highest possible level.

References: 1. *Tamás, P.:* Application of value stream mapping at flexible manufacturing systems Key Engineering Materials 686 pp 168-173, 2016; https://doi.org/10.4028/www.scientific.net/KEM.686.168.

2. *Molnár, Z., Tamás, P., & Illés, B.* (2021). The Life Cycle of the Layouts of Flexible and Reconfigurable Manufacturing Areas and Lines. Advanced Logistic Systems - Theory and Practice, 15(1), 20-29. https://doi.org/10.32971/als.2021.003. **3.** *Muther, R., Hales, L.* Systematic Layout Planning, Management & Industrial Research Publications, 2015, ISBN 978-0-933684-06-5. **4.** *Muther, R., Wheeler, J.D.* Simplified Systematic Layout Planning, Management & Industrial Research Publications, 1994, ISBN0-933684-09-6. **5.** *Kouvelis, P., and A. S. Kiran.* 1991. "Single and Multiple Period Layout Models for Automated Manufacturing Systems." European Journal of Operational Research 52 (3): 300–314. https://doi.org/10.1016/0377-2217(91)90165-R. **6.** *Moslemipour,G., T. S. Lee, andY.T.Loong.* 2017. "Performance Analysis of Intelligent Robust Facility Layout Design." Chinese Journal of Mechanical Engineering 30 (2): 407–418. https://doi.org/10.1007/s10033-017-0073-9. **7.** *Neumann, C.S.R. & Fogliatto, Flavio.* (2012). Factors that impact on increasing the flexibility of the manufacturing layout. Espacios. 33. **8.** *Moslemipour, Ghorbanali & Lee, Tian & Rilling, Dirk.* (2011). A review of intelligent approaches for designing dynamic and robust layouts in flexible manufacturing systems. The International Journal of Advanced Manufacturing Technology. 60. 10.1007/s00170-011-3614-x. **9.** *Patel, Jeemit & Patel, Karan & Manickam, Ramachandran.* (2020). Study on Various Plant Layout used in Flexible Manufacturing System.

Жолт Мольнар, Петер Тамаш, Бела Іллеш, Мішкольц, Угорщина

ВИКОРИСТАННЯ МЕТОДУ СИСТЕМНОГО ПЛАНУВАННЯ РОЗМІЩЕННЯ ОБ'ЄКТІВ ПРИ ПРОЕКТУВАННІ ГНУЧКИХ ВИРОБНИЧИХ ОСЕРЕДКІВ

Анотація. *Гнучкі виробничі системи стають все більш важливими, оскільки клієнти все частіше бажають індивідуалізованих продуктів. Крім того, тенденція до скорочення життєвих циклів продуктів викликає поширення гнучких виробничих систем. Правильне компонування - ключ до справді гнучкої виробничої системи. Нові дослідження та ця стаття показують, як метод планування системного компонування може бути застосований до проектування гнучких виробничих систем та, надалі, як процес проектування може підтримуватись моделюванням виробничого процесу. Системне планування макета переважно використовується для великих проектів. Він ділить проектування компонування на чотири основні частини та визначає точки діяльності, що визначають рух матеріалів у виробничій зоні при виробництві. Для планування компонування невеликих проектів, таких як компонування конкретного відділу або навіть групи машин, у Systematic Layout Planning є спрощена версія, яка називається «Спрощене системне планування компонування». Ця методологія може добре працювати для невеликих проектів, де матеріальний потік меши домінуючий, але розміщення окремих пристроїв та обладнання важливіше. У разі гнучких виробничих систем важливо наголосити, що з п'яти основних параметрів, продукт, кількість та маршрут можуть змінюватися досить часто. Також важливо бачити, що життєвий цикл гнучких виробничих систем може бути продовжений, у більшості випадків із запровадженням нового продукту, що означає, що система має бути підготовлена до впровадження нових елементів та нових машин протягом її життєвого циклу. У цій статті ми розглянули, як сьогодні можна використовувати методологію макетування для проектування більш гнучких виробничих систем. Поєднання методології системного планування компонування з дискретним моделюванням, керованим подіями, забезпечило ефективне та високопродуктивне проектування компонування. Подальші кроки у дослідженні будуть спрямовані на автоматизацію методології проектування максимально можливого рівня.*

Ключові слова: *системне планування компонування; моделювання; гнучкі виробничі системи.*

UDC 621.914.1 **doi: 10.20998/2078-7405.2021.95.04**

A. Nagy, J. Kundrák, Miskolc, Hungary

ANALYSIS OF THE CHANGE IN ROUGHNESS ON A FACE-MILLED SURFACE MEASURED EVERY 45° DIRECTION TO THE FEED

Abstract. *In this article, we analyze the difference (inhomogeneity) of the roughness values measured on a nonalloy carbon steel surface milled with a parallelogram-shaped (κ_r = 90°) insert as a function of the the tool movement direction and the relative position of the examining points on the workpiece surface. The characteristic distribution of roughness and the magnitude of the deviations were examined by measuring at selected points along several planes on a surface characterized by the movement conditions of the workpiece and the symmetrically arranged tool perpendicular to the machined surface, which formed double milling marks. The selected points mark the lines with specified inclinations with respect to the feed direction, and their measured values were compared. In these directions, the magnitude of the difference in roughness measures was obtained.*
Keywords: *face milling; surface roughness; distribution of roughness.*

1 INTRODUCTION

Face milling is one of the most widely used methods in the industry for machining flat surfaces, due to its high productivity, the high quality surface available and the wide use of the parts machined in this way. One of the conditions for achieving good quality is to create a topography that meets the operational requirements.

For cutting with a tool having defined edge geometry, a periodic topography is obtained, while for a cutting with an abrasive tool, a random topography is created. The theoretical impression of a tool edge having defined geometry is determined by the cutting edge angles and the magnitude of the feed rate used, measured in the tool reference plane. The more complex the motion conditions are (and the more the chip cross-section changes) in the chip removal, the more varied the theoretical profile will be, so it is justified to analyze the surface topography and explore its characteristics.

Various surface textures are created under different geometric and kinematic conditions, for which the standard ANSI Y14.36-1978 [1] also shows an example. Unlike those examples a more complex topography is created with face milling. This was analyzed by Kundrák and Felhő using a method based on CAD modeling [2], showing how to determine the roughness characteristics of the theoretical surface of a tool having defined edge geometry and the possibility of estimating and designing the desired roughness values. The significance lays in the fact that the theoretical roughness values of the face milled surface can be determined in directions other than the feed, as well as at any point on the surface. By using this, it was shown by measurements at three different locations that the roughness of the face milled surface varies from position to position [3].

In another of their articles [4] they described a method for describing the relationship between theoretical and experimental roughness indices using a defined edge geometry tool (stationary and rotary tool).

Felhő et al. [5] presented an analytical model and a test method for inserts with two different edge geometries to estimate surface roughness values in advance.

Arizmendi et al. developed another method for creating face milling surface topographic models. In one of their articles [6] the model was developed by analytical prediction of surface topography. This allows simulation analysis of roughness profiles created in different planes of the workpiece surface.

The values of experimentally determined roughness parameters are influenced by several factors in addition to the determinate characteristics of the theoretical values, the effect of which is widely studied. Chuchala et al. [7] studied the effect of the depth of cut and the number of passes on the roughness on an aluminum alloy, which was measured symmetrically arranged along the path of the milling tool axis. There was a difference in the nature of the changes in the values of the 2D and 3D roughness parameters. Furthermore, it was found that the average values of the roughness parameters were the highest on the surface part produced by down-milling.

Pham et al. [8] examined the contact length between the tool edge and the chip, the amplitude of the workpiece vibration, and the average roughness in face milling with a carbide insert on A6061 aluminum alloy. The results showed that the contact length, the degree of vibration and with it the roughness decreased with increasing cutting speed, while they increased with increasing feed rate and depth of cut.

Gocke [9] studied the effect of cutting speed and feed on surface roughness and tool wear in the face milling of martensitic stainless steel. It was found that the roughness is mainly affected by the feed and the wear by the cutting speed. Their intensity and nature differed for different inserts.

Bruni et al. [10] analyzed the effect of the lubrication-cooling condition on the roughness on stainless steel, considering the cutting time. It was found that in the case of wet cutting and MQL technique, the roughness decreased with time, while in the case of dry machining it increased slightly.

Sai et al. [11] optimized the cutting parameters to achieve the least roughness in up-face milling, during which the optimal cutting speed was determined.

Pimenov et al. [12] studied the effect of the relative position of the workpiece and the milling tool on the surface roughness. It was found that from the machined surface having an up-milled dominant part to a down-milled overwhelming part, the roughness measured in the direction of the feed rate showed a gradual increase.

The above analysis also shows that the theoretical and the real roughness values measured on the topographies of the machined surfaces may be different due to additional factors influencing the cutting process. Our goal in face milling is to explore the difference in roughness values measured at different points on the surface, in other words, the roughness inhomogeneity of the surface. This was previously addressed by

Nagy and Kundrak [13], where the change in roughness of the face milled surface was investigated by roughness measurements parallel to and perpendicular to the feed direction. In experiments it was shown that the values of the roughness parameters on the surface vary depending on the measurement direction and location. In symmetrical milling, the roughness values were influenced by which side of the symmetry plane the cutting takes place on. The difference was explained by the effect of up- and down-milling.

In this paper, we deal with the analysis of roughness values measured at points fitted to lines parallel to the feed direction and at 45° or 90° to the direction of feed.

2 EXPERIMENTAL AND MEASUREMENT CONDITIONS

2.1 EXPERIMENTAL CONDITIONS

Machine tool: PerfectJet MCV-M8 vertical milling center

Workpiece material: normalized C45 unalloyed steel

Machined surface geometry: 58 mm width, 50 mm length

Cutting tool: Sandvik R252.44-080027-15M face milling head (D_t = 80 mm)

Cutting insert: one Sandvik R215.44-15T308M-WL parallelogram-shaped coated carbide insert ($\kappa_r = 90°$, $\gamma_o = 0°$, $\alpha_o = 11°$, $r_\varepsilon = 0.8$ mm)

Cooling-lubrication: with dry cutting conditions

Cutting strategy: The surface was machined to its full width with a symmetrical setting. The edge of the tool with an axis perpendicular to the milled surface formed double milling marks on the surface, thus the front-cutting and back-cutting edge traces were also visible.

Cutting data: the cutting speed was v_c = 300 m/min, the feed rate per tooth was f_z = 0.3 mm/tooth, the depth of cut was a_p = 0.8 mm

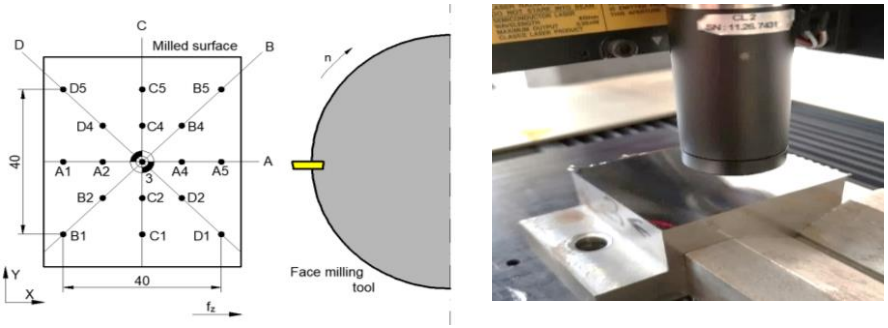

a b

Figure 1 – Analysis system of surface inhomogeneity (a), the specimen and the measuring probe (b)

2.2 ROUGHNESS MEASUREMENT CONDITIONS

Measuring equipment: AltiSurf 520 three-dimensional surface topography measuring instrument, using a confocal chromatic probe (Fig. 1b)

Evaluation software: AltiMap Premium

Measurement strategy: Measuring points were recorded on an area of 40×40 mm^2 on the machined surface so that the corresponding points designate defined examining planes. The position of the planes relative to the feed direction is shown in Fig. 1a and the positions of the points are given in Table 1, where the zero point is fitted to **A3 = B3 = C3 = D3 = 3**. Accordingly, line **A** is the symmetry plane of the surface, where the tool axis moves in the feed direction, and the other planes are rotated at a defined angle from **A** (**B** - 45°, **C** - 90°, **D** - 135°). At each point, the roughness was measured parallel to and perpendicular to the feed direction according to the requirements of ISO 4287:1997; the measurement length was 4 mm, and the cut-off length was 0.8 mm.

Table 1 – Positions of measurement points

Point	X [mm]	Y [mm]	Point	X [mm]	Y [mm]
A1	-20	0	C1	0	-20
A2	-10	0	C2	0	-10
3	0	0	C4	0	10
A4	10	0	C5	0	20
A5	20	0	D1	20	-20
B1	-20	-20	D2	10	-10
B2	-10	-10	D4	-10	10
B4	10	10	D5	-20	20
B5	20	20			

3 RESULTS

After milling the surface, the values of the roughness parameters were measured at the given points. Arithmetic mean roughness Ra and maximum height of profile Rz parameters are reported (the most commonly used parameters in the industry of the indices defined in ISO 4287). The measurements were repeated three times at each point, and the results described in Table 2 give their arithmetic mean.

$$R_i = (\sum_{j=1}^{n} R_{i,j})/n \quad (i = a, z) \tag{1}$$

The values are summarized in Table 2 to correspond with the evaluation. Thus, the numbering of the measuring points, except for plane **A**, reflects the direction of the front-cutting movement of the tool edge in the workpiece. The calculation of the average values over the whole surface is given by Equation (1), where $j = 1 \ldots n$ is the number of measuring points. Their results are R_a = 1.154 μm, R_z = 5.275 μm.

Table 2 – Roughness values in the marked direction planes

No.\Plane	R_a [μm]				R_z [μm]			
	A	**B**	**C**	**D**	**A**	**B**	**C**	**D**
1	1.10	1.56	1.53	1.50	4.94	6.84	6.77	6.50
2	1.09	1.35	1.33	1.31	4.69	5.99	5.86	5.64
3	1.13	1.13	1.13	1.13	4.83	4.83	4.83	4.83
4	1.05	0.77	0.83	0.79	4.64	4.38	4.75	4.38
5	1.01	1.06	1.13	1.02	4.66	5.42	5.36	5.01

4 DISCUSSION

The deviations of the values obtained at the measurement points from the total average are analyzed as given in Equation (2), where $j = 1 \ldots n$ is the number of measuring points. These are summarized in Table 3. The deviation values are plotted in bar graphs (Fig. 2) to assist in the evaluation method.

$$\Delta R_i = R_{i,j} - R_i \qquad (i = a, z) \tag{2}$$

Regarding the values of the deviations, it can be said that the parameters R_a and R_z show the same nature for a given plane. Since the values in the planes **B** and **D**, which are symmetric to plane **C**, have nearly the same values at the same point number, it can be concluded that one direction is sufficient to be chosen in order to characterize the roughness of the surface in the 45° direction with minimal deviations.

Table 3 – Deviations of roughness values from total average values

No.\Plane	ΔR_a [μm]				ΔR_z [μm]			
	A	**B**	**C**	**D**	**A**	**B**	**C**	**D**
1	-0.06	0.40	0.37	0.35	-0.33	1.56	1.50	1.23
2	-0.06	0.19	0.18	0.16	-0.59	0.71	0.59	0.36
3	-0.02	-0.02	-0.02	-0.02	-0.45	-0.45	-0.45	-0.45
4	-0.10	-0.39	-0.32	-0.36	-0.63	-0.89	-0.53	-0.89
5	-0.15	-0.09	-0.02	-0.14	-0.62	0.15	0.09	-0.27

The deviation values are scattered between R_a = -0.39…0.4 μm and R_z = -0.89…1.56 μm, which mean significant (70% and 47%, respectively) differences. Values in plane **A** are close to average (the highest differences from it are R_a = 0.15 μm, R_z = 0.63 μm), for the other planes, the values from the average are higher at points **1, 2** on the entry side, close to it in the middle **3** points, and smaller at point **4** on the exit side. Within a plane, the variance of the values is maximal in plane **B** (ΔR_a = 0.79 μm, ΔR_z = 2.45 μm). The least deviations can be

found within plane **A** (ΔR_a = 0.13 μm, ΔR_z = 0.3 μm), in the other directions there are differences close to the maximum. Thus, it can be concluded that large variations in the measured roughness values are expected in any examining plane with an angle other than the direction parallel to the feed.

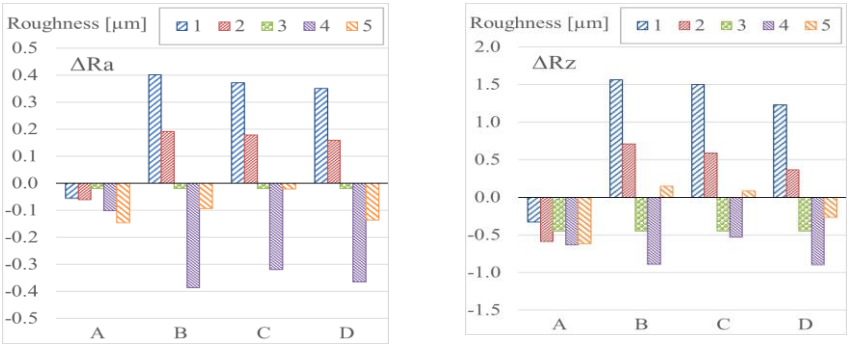

Figure 2 – Magnitude of the differences in roughn ess values in the examining planes

A relative increase in the values of point **4** is observed when the angle of the examining plane is closer to plane **C**. In each plane maximal roughness values are found in point **1** on the entry side (all the points of plane **A** are fitted to the symmetry plane, so now this is an exception), and with getting further from it, towards the exit side of the surface a decrease can be observed. However, the location of the minimum values is not on the far exit side (at point **5**). In each plane except **A** it is found that the roughness values continuously decrease in the direction of points **1** to **4**, and then on the far exit side at point **5** they increase to values that are close to the average. Also, on the entry side, the values of points **1** and **2** increase the total average, while points **3** and **4** decrease it. Based on the latter, it can be said that the values of the amplitude roughness parameters are higher on the entry side, where there is up-milling, than on the exit side, where down-milling occurs.

For the values of all points with the same number, it can be seen that if planes with angle $\propto > 0°$ are considered, they have almost the same value. The common characteristic is that the points with the given number are at the same distance from the plane of symmetry. In this regard, it can be stated that the roughness values of a measuring point – for the parameters R_a and R_z – are basically determined by how far the point is from the symmetry plane and on which side of the surface.

5 CONCLUSIONS

In this paper the change in roughness was examined at different points on the topography along several analysis planes at different angles from the feed direction on a dry face milled steel workpiece surface. At the selected points, the 2D profile roughness was measured in a direction parallel to and perpendicular to the feed. The findings are as follows.

On the 40×40 mm^2 examined area on the symmetrically face milled surface cut with a tool having a nominal diameter of D_t = 80 mm, the values of the arithmetic mean height R_a and the maximum height of profile R_z parameters scattered significantly: the magnitude of them was about 0.8 μm and 2.5 μm, which mean(s) 70% and 47% deviations, respectively. As a result, the roughness inhomogeneity of a face-milled surface is considerable, and this needs investigation.

Large deviations in the measured roughness values can be expected in any examining plane with an angle other than the feed direction.

It was found that the magnitude of the roughness values depends on the distance from the symmetry plane and the location of the point on the surface, so in a plane parallel to the feed direction, a small deviation of the values is typically expected.

The highest roughness on the machined surface was measured on the side of the surface where the tool edge enters the workpiece, where the roughness values increased the average. A minimal value was found on the exit side, where the roughness was lower than average. The values measured on the symmetry plane were close to the mean. With this it can be stated that for maximum values it is incorrect to measure the roughness of the face milled surface in the symmetry plane; according to our analysis the maximum value typically occurs on the entry side. Further studies will focus on determining its exact location.

References: 1. Surface Texture Symbols: ASME Y14.36M-1978, American National Standards Institute. **2.** *Kundrak, J., Felho, C.:* 3D roughness parameters of surfaces face milled by special tools, Manufacturing technology vol.16(3) (2016) pp.532-538. **3.** *Kundrak, J., Felho, C.:* Topography of the machined surface in high performance face milling, Procedia CIRP vol.77 (2018) pp.340-343. **4.** *Felho, C., Kundrak, J.:* Characterization of topography of cut surface based on theoretical roughness indexes, Key Engineering Materials vol.496 (2012) pp.194-199. **5.** *Felho, C., Kundrak, J.:* Comparison of Theoretical and Real Surface Roughness in Face Milling with Octagonal and Circular Inserts, Key Engineering Materials vol.581 (2014) pp.360-365. **6.** *Arizmendi, M., Jiménez, A.:* Modelling and analysis of surface topography generated in face milling operations, International Journal of Mechanical Sciences vol.163 (2019) ArtNo.105061. **7.** *Chuchala, D., Dobrzynski, M., Pimenov, D.Y., Orlowski, K.A., Krolczyk, G., Giasin, K.:* Surface roughness evaluation in thin EN AW-6086-T6 alloy plates after face milling process with different strategies, Materials vol.14(11) (2021) ArtNo.3036. **8.** *Pham, T. Nguyen, D., Banh, T., Tong, V.:* Experimental study on the chip morphology, tool-chip contact length, workpiece vibration, and surface roughness during high-speed face milling of A6061 aluminum alloy, Proceedings of The Institution of Mechanical Engineers Part B - Journal of Engineering Manufacture vol.234(3) (2020) pp.610-620. **9.** *Gocke, H.:* Optimisation of Cutting Tool and Cutting Parameters in

Face Milling of Custom 450 through the Taguchi Method, Advances in Materials Science and Engineering vol.2019 (2019) ArtNo.5868132. **10.** *Bruni, C., d'Apolito, L., Forcellese, A., Gabrielli, F., Simoncini, M.:* Surface roughness modelling in finish face milling under MQL and dry cutting conditions, International Journal of Material Forming vol.1(1) (2008) pp.503-506. **11.** *Saï, K., Bouzid, W.:* Roughness modeling in up-face milling, International Journal of Advanced Manufacturing Technology vol.26 (2005) pp.324-329. **12.** *Pimenov, D.Y., Hassui, A., Wojciechowski, S., Mia, M., Magri, A., Suyama, D.I., Bustillo, A., Krolczyk, G., Gupta, M.K.:* Effect of the relative position of the face milling tool towards the workpiece on machined surface roughness and milling dynamics, Applied Sciences vol.9(5) (2019) ArtNo.842. **13.** *Nagy, A., Kundrák, J.:* Changes in the values of roughness parameters on face-milled steel surface, Cutting & Tools in Technological Systems vol.92 (2020) pp.85-95.

Антал Надь, Янош Кундрак, Мішкольц, Угорщина

АНАЛІЗ ЗМІНИ ШОРСТКОСТІ ФРЕЗЕРОВАНОЇ ПОВЕРХНІ, ЯКА ВИМІРЮВАЛАСЬ В НАПРЯМКУ 45° ДО ВЕКТОРА ПОДАЧІ

Анотація. *У цій статті аналізується різниця (неоднорідність) значень шорсткості, виміряних на поверхні заготівки з нелегованої вуглецевої сталі, фрезерованої пластиною у формі паралелограма (κ_r = 90°), залежно від напрямку руху інструменту та відносного положення точок поверхні заготовки, що розглядаються. Характерний розподіл шорсткості і величина відхилень були досліджені шляхом вимірювання у вибраних точках уздовж декількох площин на поверхні, що характеризується умовами руху заготовки та симетрично розташованого інструменту, перпендикулярного оброблюваній поверхні, які утворювали подвійні сліди фрезерування. Вибрані точки відзначають лінії із заданими нахилами по відношенню до напрямку подачі, а виміряні їх значення порівнюються. За цими напрямами була отримана величина відмінності у показниках шорсткості. У вибраних точках була виміряна шорсткість 2D-профілю у напрямку, паралельному та перпендикулярному вектору подачі. Висновки такі. На досліджуваній площі 40 × 40 мм^2 на симетрично торцево фрезерованій поверхні, обробленій інструментом номінальним діаметром D_t = 80 мм, значення параметрів середньої арифметичної висоти R_a та максимальної висоти профілю R_z суттєво розійшлися: їх величини становили приблизно 0,8 мкм та 2,5 мкм, що означає відхилення 70% та 47% відповідно. В результаті неоднорідність шорсткості торцево фрезерованої поверхні є значною, і це потребує дослідження. Великі відхилення у виміряних значеннях шорсткості можна очікувати у будь-якій площині дослідження з кутом, відмінним від напряму подачі. Було виявлено, що величина значень шорсткості залежить від відстані від площини симетрії та від положення точки на поверхні, тому в площині, паралельній до напряму подачі, зазвичай очікується невелике відхилення значень. Найбільша шорсткість обробленої поверхні була виміряна на тій стороні поверхні, де край інструменту входить у заготовку, де середнє значення шорсткості збільшується. Мінімальне значення було виявлено на вихідній стороні, де шорсткість була нижчою за середню. Значення, виміряні на площині симетрії, були близькі до середніх. При цьому можна констатувати, що для максимальних значень некоректно вимірювати шорсткість фрезерованої торцевої поверхні в площині симетрії; згідно з нашим аналізом, максимальне значення зазвичай спостерігається на боці входу. Подальші дослідження будуть зосереджені на визначенні його точного розташування.*

Ключові слова: *торцеве фрезерування; шорсткість поверхні; розподіл шорсткості.*

UDC 621.923 **doi: 10.20998/2078-7405.2021.95.05**

R. Strelchuk, O. Shelkovyi, Kharkiv, Ukraine

RESEARCH OF THE CUTTING MECHANISM AT ELECTRICAL DISCHARGE GRINDING

Abstract. *The paper presents the results of a study of the cutting mechanism during electrical discharge grinding of hard alloys. The cutting mechanism during electrical discharge grinding was studied using mathematical modeling. By means of geometric modeling, a method of grinding cup wear was developed. The functional dependence of the diamonds use factor in the Kw wheel on the technological parameters of processing, wear and tool characteristics were determined. Analysis of the results of the study shows that an increase in efficiency at electrical discharge grinding can be achieved by reducing the wear of S, and by corresponding variation in the concentration of diamonds and technological modes of processing.*

Keywords: *mathematical modeling;wheel wear; technological modes of processing.*

Introduction. Combined processing methods can improve the performance of metal-bonded diamond wheels and expand the technological capabilities and areas of their effective application. One of these methods is the process of electrical discharge diamond grinding with a changing polarity of the electrodes over time in the cutting area [1, 2].

The intensification of the process of electrical discharge diamond grinding is carried out due to the formation of spark electrical discharges in the cutting area, which affect the processed material and the working surface of the diamond wheel on current-conducting bond, which contributes to the preservation of the high cutting capacity of the diamond wheel, as well as the stability of the relief [3].

The cutting mechanism during electrical discharge grinding of hard alloys has not been studied. In this regard, it is of interest to analyze such a process indicator as the number of active cutting grits within the contact area of the diamond-bearing layer with the processed surface. The cutting mechanism allows evaluating the qualitative side of the interaction of the processed material and the cutting surface of the tool [4]. The nature of this interaction largely depends on the technological parameters of the process, which affect the state of the working surface of the wheel and the surface layer of the part material.

Research Methodology. The cutting mechanism in electrical discharge grinding is convenient to study by modeling. To study the cutting mechanism during flat grinding with a wheel face, a geometric model of the process was chosen, and the results obtained were refined using a mathematical model [5, 6]. During the processing, the tool wears out in two directions: axial (parallel to the working surface) and radial. Axial wear of the diamond-bearing layer with thickness S_1 (Fig. 1) runs along the surface, which is formed by the helical motion of the rectilinear

generator, which is an instantaneous cutting edge.

In the considered case, the lines generating a set located on the processed surface of the part will be parallel to the cutting surface of the wheel and perpendicular to its axis. As a result, we get a surface constructed according to the height of the diamond-bearing layer, which is a helical cylinder, obtained by the motion of a rectilinear generator sliding along two helical lines of the same pitch *S* and remaining parallel to the cutting surface of the tool.

During electrical discharge grinding, electric discharges remain in force in the cutting area, and they occur when the interelectrode gap between the chip or metal surface and the bond is broken. Therefore, the radial wear of the diamond-bearing layer of the wheel with a thickness of S_2 is assumed to be equal to the value of the interelectrode gap. Since radial wear occurs simultaneously with axial wear, the wear surface takes on a curved shape created by the motion of the generator sliding along two helical lines with a pitch *S* (Fig. 2).

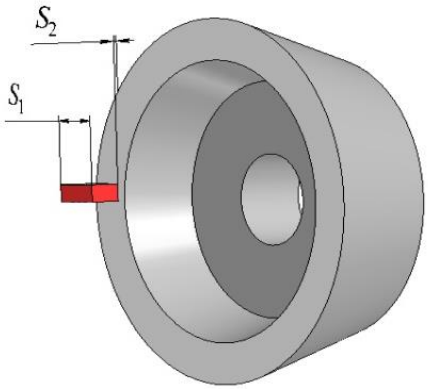

Figure 1 – Schematic diagram of the axial, radial wear of the diamond-bearing layer of the wheel

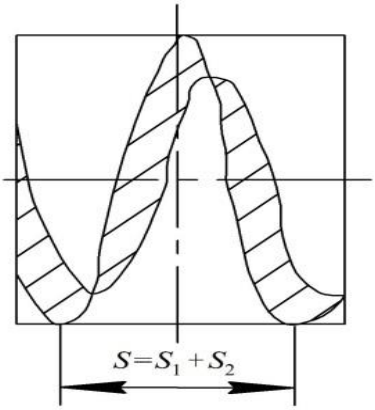

Figure 2 – Schematic diagram of formation of the surface of a helical cylinderalong the height of the diamond-bearing layer of the wheel

To determine the number of active Z_a grits directly involved in cutting, it is necessary to find their spatial (volume) distribution in the diamond-bearing layer. For this purpose, a mathematical model of the wheel working surface was developed (Fig. 3). It is based on the distribution of active grits in the volume of the working layer with a height equal to the S_1 pitch, within which the total number of diamonds Z_s is contained, including active grits in the intermediate layers Z_{s1}, Z_{s2}... Z_s.

As the Z_{s1} grits wear out, the vertices of the Z_{s2} diamonds come into operation, and so on to the point where they are fixed in the bond. As a result of the effect of electric discharges, the bond of the wheel wears out, another series of active grits is opened, and the process of exposing them in the same order is repeated in the same order by layers. If we assume that at the initial moment of cutting, the number of vertices of active grits on the surface of the diamond-bearing layer is determined by the function $Z_a=f(Z)$ given for a certain set of grits, then taking into account the accepted model, the function should be continuous for other layers of the working surface of the wheel.

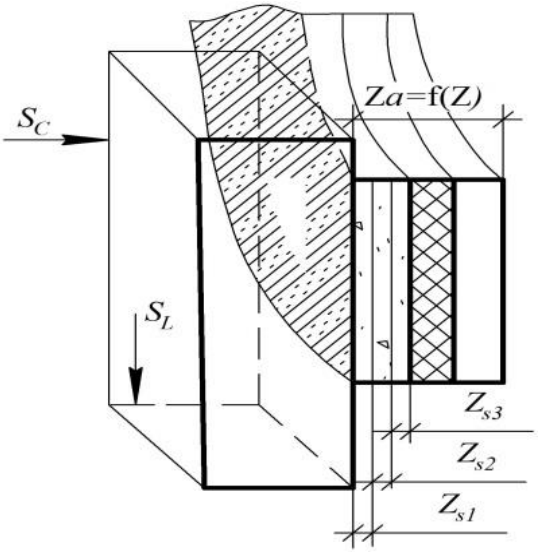

Figure 3 – Schematic diagram of the distribution of diamond grits within the cutting surface of the wheel

This is confirmed by a well-known rule in the set theory. If $Z_{1a} \in Z_{2a}$ and $Z_{2a} \in Z_{3a}$, then hence $Z_{1a} \in Z_{3a}$, i.e. this relation has transitivity. Thus, based on the transitivity property inherent in diamonds during the operation of the wheel, each of these active grits performs cutting, simultaneously wearing out, while the function $Z_a=f(Z)$ will be continuous. Provided that additional energy is supplied to the diamond wheel in the form of electrical discharges, and the grits are distributed over the volume of the working layer in accordance with the scheme shown in Fig. 3.

To determine Z_a, we first calculate the total number of Z_s grits located in the boundary layer of the working surface with S height for a grinding cup using the following ratio:

$$Z_S = 0.6 \cdot 10^6 \frac{\pi\left(R^2 - r^2\right)KS}{K_V d^3}, \quad (1)$$

where R and r, respectively, are the maximum and minimum radii of the working layer of the wheel, mm; K is abrasive concentration in the tool; K_V is the filling coefficient of the grit volume; d is the average weighted cubic grit size.

Since in this case not all the grits are of interest, but only those that are located within the cutting surface. The wear of the diamond-bearing layer of the wheel corresponding to the average grit size of the main fraction $\bar{d}$ can be taken as the pitch of the helical surface S. As a rule [7], the grits of powders, in particular diamond, are divided by size into the main (quantitatively predominant), large and small fractions. Moreover, the percentage of each of them is strictly regulated for powders of a certain grit size. Knowing the distribution of grits by fractions and calculating their total number by formula (1), it is possible to calculate their content in the diamond-bearing layer.

Results. The results of calculating the number of grits located within the cutting surface of 125×5×3 grinding cups made of diamonds of grades A, ACB and AC6 on a metal bond M1B (diamond grit size 100/80) are shown in Table 1.

Next, we determine the instantaneous number of active grits acting within the contact area F_o per rotation of the wheel.

The instantaneous shear cross section F_Z, taken by the active grits in one rotation of the wheel, is calculated by the following formula:

$$F_Z = \frac{S_C S_L H}{60 \cdot V}, \quad (2)$$

where S_C is the cross traverse of the working machine, mm/rot; S_L is the longitudinal traverse of the working machine, mm/rot; H is the height of the grinding surface, mm.

The instantaneous shear cross section can also be determined from the following expression:

$$F_Z = f_1 Z_{Fo}, \quad (3)$$

where f_1 is the shear cross section area taken by a single grit; Z_{Fo} is the instantaneous number of grits involved in cutting within the site Fo.

Table 1 – The number of grits (thousand pieces), located within the cutting surface of the wheels

Fraction	A	ACB	AC6
Large	5.8	6.1	5.1
Main	43.1	41.4	37.5
Small	15.4	13.4	8.1
Total grits	64.3	60.9	50.7

Solving equations (2) and (3) with respect to Z_{Fo}, we obtain

$$Z_{Fo} = \frac{S_C}{f_1}\frac{S_L H}{60 \cdot V}, \tag{4}$$

In the case of flat grinding with a wheel face, the cutting surface area for one rotation is expressed by the following formula:

$$F_O = \frac{\pi D S_L H}{60 V Z_a}, \tag{5}$$

Jointly solving equations (4) and (5) with respect to Z_a, we obtain the total number of active grits within the entire area of the working surface of the wheel

$$Z_a = \frac{S_C S_L H\left(R^2 - r^2\right)}{f_1 F_O 60V}, \tag{6}$$

The area f_1 can be determined by experimentally examining the chip geometry or the residual roughness of the processed surface. Since it is difficult to measure the geometric parameters of the chips due to their small sizes, the value of f_1 was found by studying the residual roughness. For this purpose, experiments were carried out on microcutting with single grit and grinding with a grinding cup with dimensions 125×10×3 AC6 125/100-M1B-100% of plates made of hard alloy BK6 with cooling.

The depth of grit penetration into the processed surface and, consequently, R_{max} are mainly determined by the cross traverse, which in the experiments varied from 0.01 to 0.06 mm/double stroke; the longitudinal traverse was 2.0 m/min, the speed of rotation of the wheel was 16 m/s. As a result of the research, an exponential

regularity of the change in the shearing section area f_1 as a function of R_{max} was established, which is expressed by the ratio $f_1 = 6.45R_{max}^{1.6}$.

Figure 4 shows the graphical dependence of the instantaneous number of Z_{Fo} grits on the cross traverse S_C. As can be seen from Fig. 4, for the described operating conditions of the wheel, the instantaneous number of active diamond grits increases with an increase in the cross traverse, since the chip removal operation and the wear of the most protruding grit vertices increase.

If at a cross traverse of 0.01 mm/double stroke the instantaneous number of diamond grits is minimal (6), then in the case of traverses of 0.05 and 0.06 mm/double stroke, it increases up to 26-28 or 4.3-4.6 times, and there is a tendency to stabilize the number of grits, which indicates that the operating conditions of the wheel are close to optimal [6].

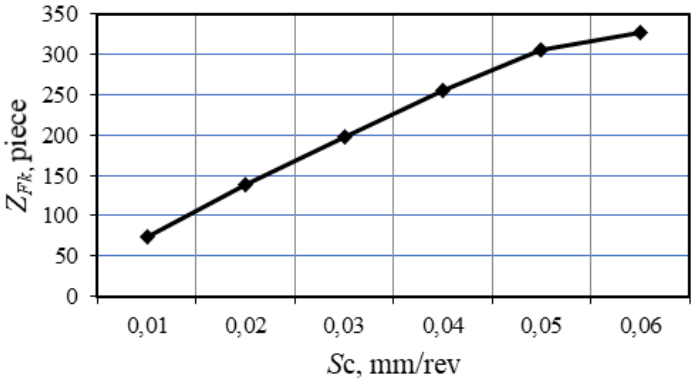

Figure 4 – Dependence of the instantaneous number of diamond grits on the cross traverse

Based on the data shown in Fig. 4, it is possible to calculate the number of active cutting grits Z_{Fk} within the contact area F_k (70 mm^2) of the diamond-bearing layer with the processed surface and, depending on the cross traverse, to estimate the diamond use factor in the wheel K_w, which is established as a result of the joint solution of equations (1), (5) and (6):

$$K_W = 0.6 \cdot 10^{-6} \frac{S_C d^3 K_V}{SK\pi D f_1}. \quad (7)$$

The values of Z_{Fk} and K_w with a cross traverse of S_C = 0.01-0.06 mm/double stroke can be taken from the graphical dependence of Fig. 5.

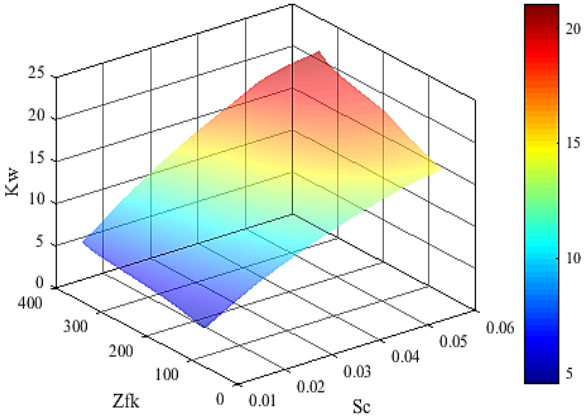

Figure 5 – Experimental values of Z_{Fk} and K_w from the cross traverse S_C.

Conclusions. The obtained results should be used when selecting the technological modes for grinding hard alloys of various grades and characteristics of diamond tools. It should be noted that even when operating under conditions close to optimal (S_C =0.06 mm/double stroke, S_L =2.0 m/min, V=16 m/s), the K_w factor is only 22.4 %, which indicates an incomplete use of the potential capabilities of diamonds in a metal-bonded wheel. This is even more evident when processing various materials in non-combined grinding conditions. According to the publications data [8, 9], about 8% of the potential cutting properties of diamond grits are used when grinding hard alloy BK8, about 12% when grinding steel, and no more than 10% when grinding cast iron.

The analysis of equation (7) shows that the increase in the efficiency of the application of diamonds in the wheel can be achieved with electrical discharge grinding due to the reduction of wear S, and the corresponding variation in the concentration of diamonds and technological modes of processing. This puts forward the task of further improving the process of electrical discharge grinding with bringing the diamond use factor to at least 40 %, as well as underlines the need for careful selection of the optimal diamond concentration in the tool and the grinding conditions.

References: 1. *Strelchuk, R., Shelkovyi, O.:* Optimization of the Interelectrode Gap in Electrical Discharge Grinding with Changing Electrode Polarity. Lect. Notes Mech. Eng. 143–152 (2021). https://doi.org/10.1007/978-3-030-77719-7_15. **2.** *Strelchuk, R., Trokhymchuk, S., Sofronova, M., Osipova, T.: Revealing patterns in the wear of profile diamond wheels. Eastern-European J. Enterp. Technol.* 3, 30–37 (2020). https://doi.org/10.15587/1729-4061.2020.203685. **3.** *Strelchuk, R.:* Investigation of the Removal of the Diamond Layer of a Wheel During Ed Grinding with Changing

Polarity of Electrodes. Ann. „Constantin Brancusi" Univ. Targu Jiu, Eng. Ser. 45–49 (2021). **4.** *Gupta, A., Kumar, H.:* Optimization of EDM Process Parameters: A Review of Technique, Process, and Outcome. In: Lecture Notes in Mechanical Engineering. pp. 981–996. Springer Science and Business Media Deutschland GmbH (2021). https://doi.org/10.1007/978-981-15-8542-5_87. **5.** *Strelchuk, R.M., Trokhimchuk, S.M.:* Mathematical modeling of the surface roughness of the grinding wheel during straightening. Nauk. Visnyk Natsionalnoho Hirnychoho Universytetu. 53–59 (2021). https://doi.org/10.33271/nvngu/2021-1/053. **6.** *Alsigar, M., Pereverzev, P., Almawash, A., Alkadhim, M.:* Optimal design of grinding systems with use of mathematical complex models ECGA. In: Materials Today: Proceedings. pp. 1521–1525. Elsevier Ltd (2021). https://doi.org/10.1016/j.matpr.2020.08.142. **7.** *Lavrinenko, V.I., Ilnitskaya, G.D., Petasyuk, G.A., Ishchenko, E. V., Gaidai, S. V., Pasichnyi, O.O., Skryabin, V. V., Shatokhin, V. V., Zaitseva, I.N., Kuz'menko, E.F., Timoshenko, V. V.:* A Study of the Potential of Improving Performance of AS20 Diamond Powders Through Altering Their Dimensional and Physico-Chemical Characteristics. J. Superhard Mater. 40, 274–281 (2018). https://doi.org/10.3103/S106345761804007X. **8.** *Zhang, Y., Li, C., Ji, H., Yang, X., Yang, M., Jia, D., Zhang, X., Li, R., Wang, J.:* Analysis of grinding mechanics and improved predictive force model based on material-removal and plastic-stacking mechanisms. Int. J. Mach. Tools Manuf. 122, 81–97 (2017). https://doi.org/10.1016/j.ijmachtools.2017.06.002. **9.** Wen, X., Cheng, J.: Experimental study of a specially designed diamond micro discontinuous grinding tool. Int. J. Adv. Manuf. Technol. 102, 3341–3356 (2019). https://doi.org/10.1007/s00170-019-03333-w.

Роман Стрельчук, Олександр Шелковий, Харків, Україна

ДОСЛІДЖЕННЯ МЕХАНІЗМУ РІЗАННЯ ПРИ ЕЛЕКТРОЕРОЗІЙНОМУ ШЛІФУВАННІ

Анотація. *У роботі наведено результати дослідження механізму різання при електроерозійному шліфуванні твердих сплавів. Механізм різання при електроерозійному шліфуванні досліджували за допомогою математичного моделювання. Шляхом геометричного моделювання розроблено методику зносу шліфувального круга чашкової форми. Визначено функціональну залежність коефіцієнта використання алмазів у крузі K_w від технологічних параметрів обробки, зносу та характеристик інструменту. Аналіз результатів дослідження показує, що підвищення ефективності при електроерозійному шліфуванні можна досягти за рахунок зменшення зносу S і відповідним варіюванням концентрації алмазів і технологічних режимів обробки. Підвищити працездатність алмазних кругів на металевих зв'язках та розширити технологічні можливості та галузі їх ефективного застосування дозволяють комбіновані методи обробки. Одним з таких способів є процес електроерозійного алмазного шліфування зі змінною полярністю електродів у часі в зоні різання. Інтенсифікація процесу електроерозійного алмазного шліфування здійснюється за рахунок утворення в зоні різання іскрових електричних розрядів, що впливають на оброблюваний матеріал і на робочу поверхню алмазного круга на струмопровідній зв'язці, що сприяє збереженню високої ріжучої здатності алмазного круга, стійкості рельєфу. Механізм різання при електроерозійному шліфуванні твердих сплавів не вивчений. У зв'язку з цим цікавий аналіз такого показника процесу, як кількість активних ріжучих зерен в межах площі контакту алмазоносного шару з оброблюваною поверхнею. Механізм різання дозволяє оцінити якісну сторону взаємодії оброблюваного матеріалу та різальної поверхні інструменту. Характер цієї взаємодії багато в чому залежить від технологічних параметрів процесу, що впливають на стан робочої поверхні круга та поверхневого шару матеріалу деталей.*

Ключові слова: *математичне моделювання; знос круга; технологічні режими обробки.*

UDC 621.9.042 **doi: 10.20998/2078-7405.2021.95.06**

O. Yakimov, S. Uminsky, N. Klimenko, K. Kirkopulo,
A. Pavlyshko, V. Vaysman, Odessa, Ukraine

IMPROVING GRINDING OF GEAR WHEELS APPLIED IN GEARBOXES OF POWER ENGINEERING

Abstract. *Development of modem power engineering follows the line of continuous increase in speed, coefficient of corrosive action and capacity of units. Gears and reducers are responsible parts of modem machinery and occupy an important place in the domestic power engineering construction. Durability and wear resistance of gears, apart from the design factors, also depends on the technological methods of treatment. The final stage of production of such wheels is the operation of gear grinding. In the process of gear grinding in a thin surface ball there are complex thermomechanical processes. As a result of short-time heating to high temperatures, structural transformations, burns, and in some cases even micro- and macro-thicknesses occur in such a surface bail. In addition, there are cases of making tooth wheels with adjacent defects grinding (for example, the appearance of the surface of the ball teeth of large tensioning forces), which reduces the life of the work, and in some cases causes a breakdown of the teeth in operating conditions. Development of effective measures to ensure the quality of the surface of the ball on the operation of grinding baggage in part depends on the possibility of predicting (or calculation) of temperatures and residual loads on the depth of the cemented teeth ball. The method of calculation of internal surplus Toads occurring during grinding of wheels with cemented steels is suggested. On the basis of the performed calculations and experiments the ways to improve the quality of production of working surfaces of gears, which are used in the wits of thermal and nuclear power plants are suggested and grounded.*
Keywords: *cemented bal; surplus load; hard masti; overpowering circle.*

Introduction. Development of modern power machine building follows the line of non- variable increase of speed, coefficient of corrosive action and capacity of units. In all cases where the optimal number of rotations of the unit motor differs significantly from the number of rotations of the operating mechanism, a gear reducer is used. Particular gears and reducers are crucial pats of modem mechanics and occupy an important place in ate of the-art power engineering. Durability and wear resistance of gears, in addition to design factors largely depends on the technological methods of processing.

Issue. Heavy-duty gear wheels are produced from cemented chromium-molybdenum and chromium-molybdenum-tungsten steels 12XH3A, 12X2H4A, 20X2H4A and 18X2H4MA. The final stage of production of such wheels is operation gear grinding. In the process of gear grinding in a thin surface ball there are complex and unique thermomechanical processes. As a result of short-term heating to high temperatures in the surface of the ball structural transformations occur, the so-called bums, and in some cases even micro and macro cracks.

Moreover, there are cases of toothed wheels produced with adjacent defects grinding (eg, the appearance of the surface ball teeth of large tensioning forces), which reduces the service life, and in some cases leads to a breakage of teeth in operating conditions. The development of effective measures to ensure the quality of the surface ball in the grinding operation depends in part on the possibility of predicting (or calculating) temperatures and residual loads on the depth of the cemented tooth ball.

Analysis of recent studies and publications. Mathematical modeling of thermal and strain-deformed state of the part material during grinding is the subject of the works [1-6]. Analytical determination of the values of deflecting residual stresses, taking into account the nonuniformity of carbon content in a grinded ball has not been given sufficient attention. The works [7, 8] analyze the causes of surface bums and cracks during grinding of cemented gear wheels. In these works the adverse effects of grinding are proposed to reduce by optimizing the parameters of the cutting mode, and the formation of the stress-strain state of the surface ball during abrasive machining is considered mainly from the qualitative side or is, devoted to experimental study of the residual stresses.

Research Objective. To develop a method for calculating temperatures and residual stresses at different levels of the cemented ball, which occurs during grinding, and to suggest ways to improve the thermal and resilient-deformed state of the tooth surface ball in abrasive machining.

Materials and methods of research.

The general technique of researches was built on the basis of scientific bases of technology of mechanical engineering with attraction of the device of chemical thermodynamics, theory of vibration, and also on the basis of scientific representations on mechanics and thermal physics of processes of cutting. Experimental researches on comparative estimation of working ability of solid, discontinuous and discontinuous impregnated abrasive wheels were carried out on the surface grinding machine of 3G71M model. As investigated materials were used flat samples in the form of parallelepipeds with the sizes 150 * 20 * 10 mm from steel U10. During the experiments, wheels with dimensions of 200 * 20 * 76 mm and characteristic 24A 40 CM2 7 K6 were used. Impregnating composition included oleic acid, acetamide and stearic acid.

Results of investigations. In the surface balls of cemented parts at grinding form stresses of different magnitude and sign. Residual stresses occur as a result of the interaction of plastic and plastic-deformed balls. If plastically deformed balls after cooling tend to increase their length in relation to their output length, then the plastically deformed balls tend to return to their output length. Thus, some of the balls will feel the tensile stress and others will feel the retracting stress. These loads remain in the part after grinding and therefore are called gaps. The main

disadvantage of grinding is the occurrence of residual stresses of considerable magnitude, which can lead to cracking the surface of the cement bead. The reason for the occurrence of gapped stresses in the grinding process at an uneven phase-structural composition of the cemented ball is the grinding temperature, which leads to a nervous thermal expansion of its individual microspheres, which causes the occurrence of gapped stresses. When calculating the grinding temperatures two conditions must be taken into account: 1. Heat flux intensity is nervously distributed along the contact surface of the grinding wheel with the workpiece. At the beginning of the trajectory of passing the rust grain in the processed material the intensity of the heat flux is less, and at the end of the trajectory, where the overflow of chips is maximal, it is higher Thus, it is necessary to determine the temperature of the cutting surface taking into account the power of the heat fix, nervously dispersed on the contact surface of the grinding wheel with the metal. 2. It is of practical interest to determine the temperatures that occur not only on the cutting surface (i.e. on the surface where the chip formations currently taking place) but also on the ground surface located below the cutting surface. In addition, for the calculation of the thermal surplus loads it is necessary to know how the temperatures of the globe of the cement ball are distributed. To solve the first problem, we select the coordinate system X,Y, Z on the surface of the bulked body. We assume that heats supplied to a certain region circumscribed by a rectangle, the sides of which are parallel to the axes X and Y:

$$-a \le x \le a,\ -b \le y \le b,\ \text{де}\ a = \frac{\sqrt{D_{kp} \cdot t}}{2},\ b = \frac{S}{2},$$

D_{kp}- diameter of the grinding wheel, t - depth of grinding, S - cross feed rate. Outside this area, there is no heat flow through the workpiece surface. Grinding depth, - transverse flow. Beyond this area, there is no heat flow through the workpiece surface. Heat source is considered non-perturbable, and the surface of the processed part is tom at a rate of speed V_∂ in the direction of decreasing coordinate x. Let us consider a tired thermal regime when $\tau \to \infty$. For an elementary plane $D = dx \cdot dy$ with the center with coordinates x, y the temperature distribution is described by dependence [9]:

$$T_1(z) = \frac{q(x)}{2\pi\lambda_1} \cdot \frac{1}{R} \exp\left(-\frac{V_\partial \cdot r + V_\partial \cdot (x_0 - x)}{2a_1\tau} \right), \quad (1)$$

where T_1 - temperature on the cutting surface, °C; *x, y, z* - current coordinates of the part position, m; $q(x)$– thermal flux intensity in the given point at the contact point of the grinding wheel with the part, Bm/m^2; λ_1 – coefficient of heat conductivity of the cutting surface, W/m·°C;

$$R = \sqrt{(x_0 - x)^2 + (y_0 - y)^2 + z^2},$$

Radius-vector of coordinates; V_∂ – velocity of moving the part over the intact thermal source, m/min; τ – moment of time, s; x_0 – coordinate at the moment of τ_0, m; r – radius of rounding of cutting grain, m; a_1 – coefficient of thermal conductivity of cutting surface, m^2/s. By interpolating the expression (1) by area D, we obtain:

$$T_1(z) = \frac{1}{2\pi\lambda_1} \int_{-a}^{+a} q(x)dx \int_{-b}^{+b} dy \left\{ \frac{1}{R} \cdot \exp\left[-\frac{V_д r + V_д (x_0 - x)}{2a_1 \tau} \right] \right\}, \quad (2)$$

where a, b – half-width and full-width of the circle contact beaches with the piece, m.

To solve the second problem, i.e. to bring the temperature at the top of the cutting to the temperature of the machined surface, it can be imagined that on this surface a body is driven, heated to temperature T_1 and composed of the material of the part, abrasive grit and the bonding of the stake. Each point of the ground surface is in contact with the body during the interval of time $\tau = \frac{\sqrt{D_{kp} \cdot t}}{V_\partial}$. In order to simplify the problem, we can assume that two interposed bodies with thermally insulated surfaces are brought into contact with each other at the initial moment of time. The temperature of the first body is equal to the temperature of the cutting surface T_1, and the temperature of the second body is equal to the temperature of the crushed surface T_2. It is necessary to find the temperature of the other body at the time from $\tau = 0$ to $\tau = \frac{\sqrt{D_{kp} \cdot t}}{V_\partial}$.

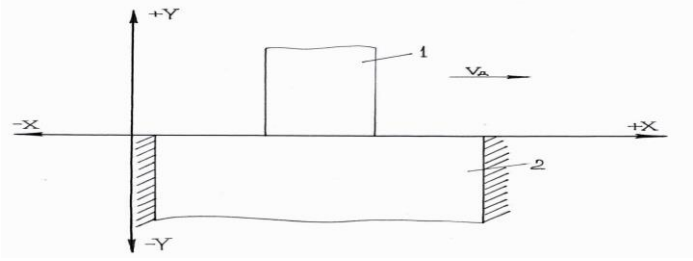

Figure 1 – Scheme for temperature calculation on the treated surface:
1 and 2 – bodies having at the initial moment of time the temperatures equal to the temperature of the cutting surface and the treated surface accordingly

Thus, the problem is reduced to the solution of the heat transfer function at the boundary conditions of the 4th type, which corresponds to the contact of two solids with different temperatures. The difference heat transfer equation is written as follows:

$$\begin{cases} \dfrac{\partial T_1(z,\tau)}{\partial \tau} = a_1 \cdot \dfrac{\partial^2 T_1(z,\tau)}{\partial z^2} & \text{at } \tau \geq 0; z \geq 0 \\ \dfrac{\partial T_2(z,\tau)}{\partial \tau} = a_2 \cdot \dfrac{\partial^2 T_2(z,\tau)}{\partial z^2} & \text{at } \tau \geq 0; z \leq 0 \end{cases} \quad (3)$$

Boundary conditions:

$$\begin{aligned} & T_1(z,0) = f_1(z); T_2(z,0) = f_2(z) \\ & \frac{\partial T_1(+\infty,\tau)}{\partial z} = \frac{\partial T_2(-\infty,\tau)}{\partial z} = 0 \\ & T_1(+0,\tau) = T_2(-0,\tau) \\ & \frac{\partial T_1(0,\tau)}{\partial z} = -\frac{\lambda_2}{\lambda_1} \cdot \frac{\partial T_2(0,\tau)}{\partial x} \end{aligned} \quad \text{at, } 0 \leq \tau \leq \frac{\sqrt{Dt}}{v_д} \quad (4)$$

where λ_2 – is the coefficient of heat conductivity of the treated surface, W/m·°C. Using Laplace transformation, we reduce the system (4) of differential equations to a system of algebraic square equations. The solution for the representation looks like:

$$\begin{aligned} & T_{L1}(z,s) - \frac{T_{01}}{s} = B_1 \exp\left(-\sqrt{\frac{s}{a_1}} z\right), \quad z \geq 0 \\ & T_{L2}(z,s) = B_2 \exp\left(-\sqrt{\frac{s}{a_2}} |z|\right), \quad z \leq 0 \end{aligned} \quad (5)$$

where a_2 – coefficient of temperature penetrability of the treated surface, m^2/s. The residual solution for the images will be:

$$\begin{aligned} & T_{L1}(z,s) = \frac{T_0}{s} - \frac{T_0}{(1+K_\varepsilon)s} \exp\left(-\sqrt{\frac{s}{a_1}} z\right), \quad z \geq 0 \quad , \\ & T_{L2}(z,s) = \frac{K_\varepsilon T_0}{(1+K_\varepsilon)s} \exp\left(-\sqrt{\frac{s}{a_2}} |z|\right), \quad z \leq 0 \end{aligned}$$

where $K_\varepsilon = \frac{\varepsilon_1}{\varepsilon_2} = \frac{\sqrt{\lambda_1 c_1 \gamma_1}}{\sqrt{\lambda_2 c_2 \gamma_2}}$ – the ratio of coefficients of thermal activity of dosed bodies, the heat source and the crushed surface.

Going to the tables of images, we have:

$$\frac{T_2(z,\tau) - T_{02}}{T_{01} - T_{02}} = \frac{K_\varepsilon}{1 + K_\varepsilon} erfc \frac{|z|}{2\sqrt{a_2 \tau}}$$

Or $T_2(z,\tau) = (T_{01} - T_{02}) \frac{\varepsilon_1}{\varepsilon_2 + \varepsilon_1} erfc \frac{|z|}{2\sqrt{a_2 \tau}} + T_{02}$ Considering, $T_{02} = 0$ we'll get it: $T_2(z,\tau) = \frac{T_{01}\varepsilon_1}{\varepsilon_2 + \varepsilon_1} erfc \frac{|z|}{2\sqrt{a_2 \tau}}$. considering, that $erfc = (1 - erf)$ we get:

$T_2(z,\tau) = \frac{T_{01}\varepsilon_1}{\varepsilon_2 + \varepsilon_1}\left(1 - erf \frac{|z|}{2\sqrt{a_2 \tau}}\right)$, where $T_{01} = T_1$ – is the temperature at the cutting surface, ·°C.

Thus, in view of the temperature on the cutting surface (2), the grinding temperature $T_2(z,\tau)$, is reduced to the machined surface, which takes into account that the power of the thermal source is nervinetrically distributed along the contact, beach and the grinding wheel on the workpiece and the thermal power at this point of the contact beach depends on the specific coordinate *x*, and is equal to:

$$T_2(z,\tau) = \frac{\varepsilon_1 \cdot \int_{-a}^{+a} q(x)dx \int_{-b}^{+b} dy \left\{ \frac{1}{R} \cdot \exp\left[-\frac{\mathbf{v}_д r + \mathbf{v}_д (x_0 - x)}{2a_1 \tau} \right] \right\}}{2\pi\lambda_1(\varepsilon_2 + \varepsilon_1)} \left(1 - erf \frac{z}{2\sqrt{a_2 \tau}}\right), \qquad (6)$$

where $\varepsilon_1, \varepsilon_2$ – coefficients of thermal activity according to the thermal source and the treated surface, W/m^2·°C.

The magnitudes of the residual pressures that occur at different levels of the cement ball can be determined by correlating with the equation:

$$G_2(z) = \frac{E_2 \alpha_2 \varepsilon_1 \int_{-a}^{+a} q(x)dx \left\{ \frac{1}{R} \cdot \exp\left[-\frac{V_\partial^2 r + V_\partial^2 (x_0 - x)}{2 \cdot a_1 \cdot \sqrt{D_{kp} \cdot t}} \right] \right\} \left(1 - erf \frac{z \cdot \sqrt{V_\partial}}{2\sqrt{a_2 \sqrt{D_{kp} \cdot t}}}\right)}{(2 - 2 \cdot \mu_2) \cdot 2\pi\lambda_1(\varepsilon_2 + \varepsilon_1)} \qquad (7)$$

where E_2 - modulus of the cement ball, Mpa; α_2 – linear coefficient of thermal expansion of the cement ball, 1/°C; μ_2 – Poisson's coefficient of the cement ball. The figure 2 shows the calculated curves describing distribution of inner loading

by the depth of the cemented ball after grinding of 18X2H4BA steel at the cutting thickness $t = 0{,}1$ mm (without cooling) and ¢= 0,015 in mm $t = 0{,}015$ mm (with cooling). From the graphs it is seen that in the measure of distance from the surface the tensioning forces decrease and pass into constraining ones. When grinding in the most severe mode (curve 2), the tightening resistances have the lowest value. The appearance of tensioning forces during grinding of gear wheels leads to a reduction of their total strength.

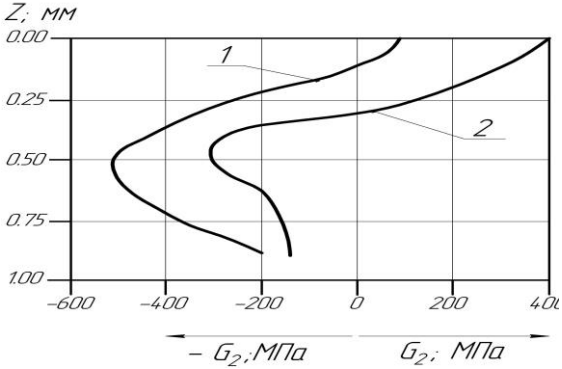

Figure 2 – Distribution of intrinsic surplus loads by the depth of the cement ball for two grinding modes: *t* = 0,015 mm and *t* =0,1mm

Thermal and physical parameters of the treated material depend on the amount of carbon in the cement ball. Carbon in the cement ball is nervously distributed (Fig. 3). [8].

Figure 3 shows that increasing the concentration of carbon in the surface ball reduces the thermal conductivity (*a*) and thermal conductivity (λ) of the treated material. Calculation of internal residual stresses was carried out taking into account the graph s $a = f(c)$, $\lambda = f(c)$. The appearance of grinding cracks is caused not only by filling and retention stresses, which occur during grinding and grinding when the temperature is cooled down to the martensitic transformation start point [11].

The reason for the formation of cracks are high contact temperatures and temperature gradient in the cutting zone, as well as high speeds of cooling the machined surface after the exit of its zone of contact with the abrasive wheel. In order to reduce the internal tensioning forces and the probability of fracture

formation, it is necessary to reduce the temperature in the cutting zone and the speed of cooling by all available means [11].

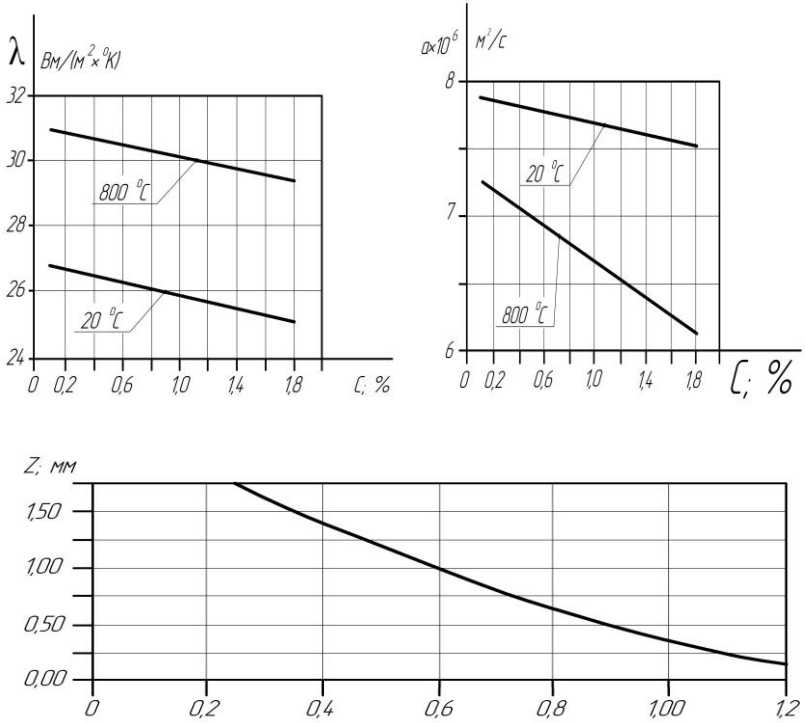

Figure 3 – Dependence of thermophysical parameters (a, λ) of 18X2H4BA steel on the amount of carbon in the surface ball [10] at different temperatures and distribution of carbon over the depth of the cement ball [8]

This can be achieved by using as a coating and cooling agent a solid lubricant [12] whose components are taken in the following proportions: stearic acid (60 - 65%), oleic acid (20 - 25%), acetamide (others). The proposed lubricant, having a high sinking ability, significantly reduces the contact temperature of grinding at a very low speed of cooling of the surface balls of parts, which provides a reduction of internal tensioning forces occurring in the process of grinding [12]. Another effective way to reduce the contact temperature can be overflow grinding [13]. Under certain conditions, operation of a grinding wheel with an intermittent working surface can cause parametric resonance in the workbench rod system,

which reduces the quality of the surface ball of the machined part. Parametric instability of the grinding machine rotary system is determined by the condition[14]

$$|L| > \frac{M+1}{2} \tag{8}$$

where L and M – parameters depending on the weight and rigidity of the rotary system of the workbench, the rheological capacity of the grinding wheel, number and sizes of pits and cutting protrusions on the working surface of the abrasive tool, the diameter and circumferential speed of the wheel, as well as the parameter characterizing the damped oscillations in time. Fig. 4 shows the areas of parametric stiffness of the workbench grinding system (flat colored plots) designed for intermittent grinding without using icing devices (two left space graphs) and with the use of solid lubricant (two right space graphs). Expansion of zones of stable work of the workbench's trunnion system at grinding with the use of solid abrasive is explained by the improvement of cutting ability of the abrasive tool in comparison with "dry" grinding. From the placement of two spatial graphs, rooted in the bottom of Fig. 4, it follows that the interval of change in the number of cutting interventions on the interval stake $5 \le n \le 20$ the size of areas stable work at grinding with a solid matrix at 35% more than for "dry" grinding. The area of these areas increased due to the reduced area of unstable work zones of the workbench system, i.e. due to the reduced area of the "hump" supports, which lie in the area described by the parameter $\frac{M+1}{2}$ (the right part of the nervousness (8)). Fig. 5 shows the experimental data on the measurement of loss of metal per hour unit K. The experiments were carried out on the surface grinding machine of model ZG71M. Samples of the steel U10 were ground by dry, overfed (n = 12, N= 0,6) and overfed by PP 250□20□76 24A 25CM2 6K5 wheels according to the parallel scheme (without the cross feed). The composition of the impregnator included stearic acid (60%), oleic acid (20%), acetamide (20%).

Fig. 5 shows that during the initial period of time the metal atomic $(0 \le \tau \le 3)$ capacity was approximately the same for three investigated processes, and after the 18-minute grinding period the tensile strength of the grinding wheel became two times lower in comparison with the overexpanded and overprepared wheel.

Decrease in rust performance of the grinding wheel is accompanied by an increase in thermal stress of the grinding process and, as a result, formation of large internal residual stresses on the machined surface.

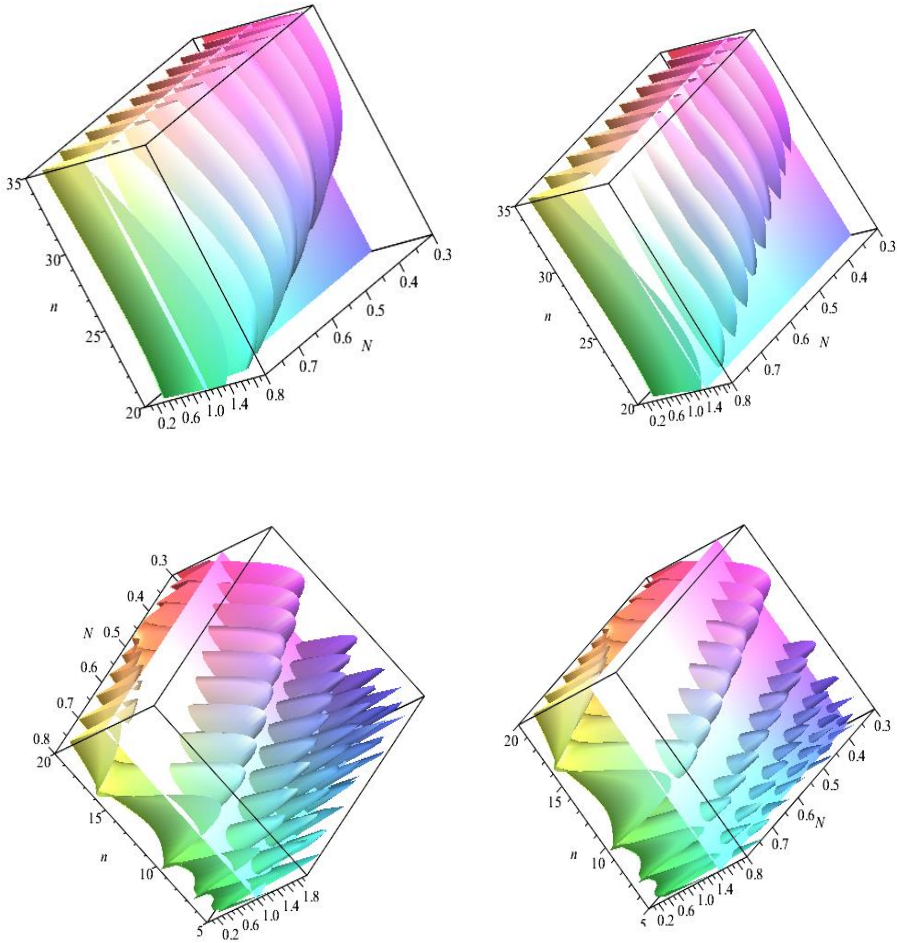

Figure 4 – Spatial graphs of dependence of parameters L and $|L| > \frac{M+1}{2}$ on the number of cutting inserts on the abrasive stake and the value of the ratio of the stock width to the protrusion length: left- for "dry" grinding; right-hand - for grinding with the use of solid lubricant.

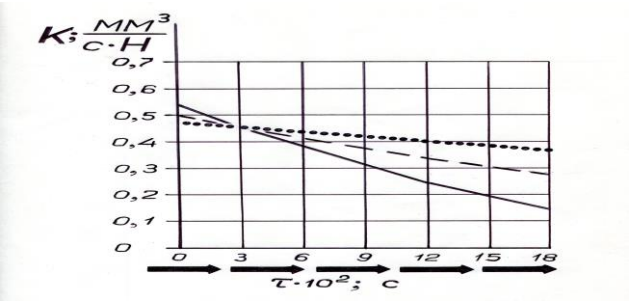

Figure 5 – Comparative estimation of the richer performance of the dry (non-interrupted line), over-interrupted (dashed line) and over-interrupted impregnated (dotted line) quill in time

Results. The method of calculation of internal residual loads occurring at grinding of wheels with cemented steels has been developed. On the basis of the performed calculations and experiments the ways to improve the quality of production of working surfaces of gears, which are used in the units of thermal and nuclear power plants are suggested and grounded.

References: 1. *Korchak S.N.* Theory of machinability of steels and alloys during abrasive machining / S.N. Korchak // Vestnik of South Ural State University: Collection of scientific works (Series "Mechanical Engineering"). – 2003. – №9. Vol.4 – pp. 82–90. **2.** *Viadimir Lebedev, Natalia Klimenko, Y. Uryadnikova, and other.* Determination of the amount of heat released when cutting metal with an abrasive grain and the contact temperature of the ground surface. East European Journal of Advanced Technologies.-Ukrainian State University of Railway Transport, 2016. – N25(7). – pp. 43–50. **3.** *Lebedev Vladimir, Klimenko Natalia, Uryadnikova Inga, and other.* Martensitic transformations in surface layer during grinding of hardened steel parts. East-European Journal of Advanced Technology, 2017 – Vol. 3, №12(87). **4.** *Melnikova, E.P.* Influence of technological factors of finish abrasive machining on surface quality / E.P. Melnikova //Technology of Mechanical Enginee ing. – 2003. – №3. – pp. 13–16. **5.** *Usov A.V., Kunitsyn M.V.* Possibilities of increasing the operational characteristics of the working surfaces of cylinders by technological methods. Bulletin of Kharkiv National Technical University. – Kherson National Technical University, 2018. – №2–3(66). **6.** *Usov A.V.* Mathematical Modeling of Linear Non Homogeneous Systems by Methods of Singular Integral Equations. Journal of the Kherson National Technical University. – 2017. – №3(1), pp. 100–104. **7.** *Genkin M.D.* Enhancement of reliability of heavy loaded gears / M.D. Genkin, M.A. Ryzhov, N.M. Ryzhov. – Moscow: Mechanical engineering, 1981. – 232 p. **8.** *Sataradze V.S.* Increasing the reliability of cemented parts / V.S. Sataradze. – Moscow: Mechanical engineering, 1975. – 216 p. **9.** *Redko S.G.* Processes of heat formation when grinding metals / Saratov: Saratov University Press, 1986. – 231p. **10.** *Bakhvalov V.A.* Research of influence of parameters of the process of gear grinding by cone wheel and input state of material on quality of surface layer: Ph. D. in Technical Sciences: 05.02.08 / – Odessa, 1977. – 350 p. **11.** *Oleksiy Yakimov, Liubov Bovnegra, Vladimir Tonkonogyi, Vladyslav Vaysman,*

Victor Strelbitskyi, Inna Sinko. Influence of the Geometric characteristics of the discontinuous profile working surfaces of abrasive wheels for precision and temperature during Grinding. Cutting and Tools in Technological Systems. – Khpi, 2021, №94. – pp. 115–125. https://doi.org/10.20998/2078-7405.2021.94.13. **12.** *Tonkonogyi Vladimir, Sidelnykova Tetiana, Dasic Predrag, Yakimov Alexey, Bovnegra Liubov*. (2020). Improving the Performance Properties of Abrasive Tools at the Stage of Their Operation. |. Karabegovic (Ed.): NT 2019, LNNS 76, pp. 136–145, 2020. https://doi.org/10.1007/978-3-030-18072-0_15. **13.** *Vladimir Tonkonogyi, Alexey Yakimov, Liubov Bovnegra, Tetiana Sidelnykova, Predrag Dasic*. The use of intermittent wheels, impregnated by the contact method to reduce the thermal stress of the grinding process/thansbud–2019. IOP Conf. Series: Materials Science and Engineering. pp. 1–11. 708(2019)012034, https://doi.org/10.1088/1757-899X/708/1/012034. **14.** *F.V. Novikov, V.A. Zhovtobryukh, V.S. Gusarev, V.B. Naddachin, A.A. Yakimov, A.A. Andilakhai, A.S. Sergeev, D.F. Novikov* Innovative development of modern technologies: monograph /. – Dnipro: Lira, 2021. – 480 p. ISBN 978-966- 981-519-4.

Олексій Якімов, Наталія Кліменко, Катерина Кіркопуло,
Андрій Павлишко, Сергій Уминський, Владислав Вайсман, Одеса, Україна

ЗАБЕЗПЕЧЕННЯ ЯКОСТІ ШЛІФУВАННЯ ЗУБЧАСТИХ КОЛІС, ЩО ВИКОРИСТОВУЮТЬСЯ В РЕДУКТОРАХ ЕНЕРГЕТИЧНОГО МАШИНОБУДУВАННЯ

Анотація. *Розвиток сучасного енергомашинобудування йде по лінії неперервного підвищення швидкостей, коефіцієнта корисної дії та потужностей агрегатів. І це безумовно призводить до інтенсифікації використання механізмів. Зубчасті передачі та редуктори є відповідальними частинами сучасних механізмів і займають важливе місце у вітчизняному енергомашинобудуванні. Міцність і зносостійкість зубчастих передач, крім конструктивних факторів, залежить і від технологічних прийомів обробки. Заключним етапом виготовлення таких коліс є операція зубошліфування. В процесі зубошліфовання в тонкому поверхневому шарі відбуваються складні термомеханічні процеси. В результаті короткочасного нагрівання до високих температур в такому поверхневому шарі виникають структурні перетворення, прижоги, а в деяких випадках навіть мікро і макротріщіни. Крім того, мають місце випадки виготовлення зубчастих коліс з прихованими дефектами шліфування (наприклад, появлення в поверхневому шарі зубів великих розтягуючих напруг). Це призводить до того, що знижується ресурс роботи механізмів, а в окремих випадках може викликати пошкодження зубів (в тому числі, призвести до поламки) в умовах експлуатації. Розробка ефективних заходів по забезпеченню якості поверхневого шару на операції зубошліфування багато в чому залежить від можливості прогнозування (або розрахунку) температур і залишкових напружень по глибині цементованого шару зубів. Запропоновано методику розрахунку внутрішніх залишкових напружень виникаючих при зубошліфуванні коліс зі сталей, що цементуються. На основі виконаних розрахунків і експериментів було запропоновано, а також наведено обгрунтування щодо шляхів підвищення якості виготовлення робочих поверхонь зубчастих передач, що застосовуються в агрегатах теплових і атомних електростанцій.*

Ключові слова: *цементований шар; залишкові напруження; тверде мастило; переривчастий шліфувальний круг.*

UDC 621.91.01 **doi: 10.20998/2078-7405.2021.95.07**

O. Koval'chuk, V. Nezhebovsky, O. Permyakov,
O. Klochko, Kharkiv, Ukraine, S. Ryabchenko, Kyiv, Ukraine

PROCESSING OF HARDENED CYLINDRICAL GEAR WHEELS OF THE CUTTING GEARBOX OF THE COMBINE UKD 200-500

Abstract. *The article discusses the latest developments of unique technological methods of gear milling of cylindrical gears for preliminary blade gear processing of hardened cylindrical gears of the cutting reducer of the UKD200-500 coal mining harvester for the final gear grinding of gear teeth with modulus m = 16 mm, with hardness HRC 56 ... 62. The peculiarity of the design of special hob cutters is that a circle passing through the lower boundary points of the involute is used as the palloid of the machine gearing of the tool and part. Pre-cutting the teeth of hardened wheels with carbide milling cutters allows you to remove the main allowance for the final gear grinding.*
Keywords: *hardened wheels; preliminary blade gear machining; high-speed gear hobbing; technological methods.*

1. INTRODUCTION

Increasing the efficiency of industrial production is largely associated with the development of mining equipment, transport, energy systems of machines, the drives of which contain large-scale gear drives (m = 12 ... 30mm). The bearing capacity of gearwheels in terms of contact strength increases with the surface hardness of the teeth. Increasing the hardness of the surface of the teeth from HRC32 to HRC62 makes it possible to halve the dimensions of the gearbox and reduce the mass by 3 times.

The high requirements for reliability and strength are presented to the cylindrical gearwheels of the cutting reducer of the UKD200-500 combine harvester. However, the high labor intensity of manufacturing cemented hardened coarse-modular gears due to significant allowances assigned for gear grinding operations to eliminate defects after heat treatment, the possibility of burns and micro cracks that contribute to the formation of macro cracks and chipping of teeth requires a scientific approach in solving problems of processing hardened gears. A unique technology for the manufacture of hardened coarse-modular gears of a high degree of accuracy with preliminary cutting of teeth for carburizing and hardening with subsequent removal of the main allowance to 95% with a special blade tool and final gear grinding with a minimum allowance of 5% has been proposed.

2. PURPOSE AND OBJECTIVES

For processing coarse-modular gears with high wear resistance of the teeth, with high strength properties of the surface layer, it is advisable to study the

technological directions of processing hardened coarse-modular gears to ensure the necessary parameters of surface roughness, gear hobbing quality with the achievement of high productivity, accuracy and quality of gear processing of hardened coarse-modular gears, due to improvement of technology and kinematics of gear milling, development of instrumental and technological equipment, which will ensure the predicted quality of the surface layer of the teeth and the performance properties of the gears. To achieve this goal, the following research objectives have been identified:

– to analyze and establish the main directions of increasing the productivity and quality of gear processing of hardened large-modular gear wheels in the conditions of small-scale production;

- to substantiate the application of technological methods of gear processing:

- to formulate the criteria for choosing the structure and parameters of the systems for blade processing of hardened coarse-modular gears in order to ensure the specified operational properties.

3. MATERIALS AND METHODS

Unique technological methods of preliminary blade gear processing of hardened spur gears of coal miners' reducers provide for preliminary blade gear cutting to remove the main allowance of 95%, followed by gear grinding when removing the final allowance of 5% gear wheels with modulus m = 16 mm, , with hardness HRC 56... 62. The complex of scientific research works with the development of original technological processes, prospective constructions of worm carbide cutters, special technological equipment was made. Technological regulations have been developed and implemented for the high-speed gear hobbing with blade carbide cutters with a final clean slash operation by applying effective grinding technologies.

The special worm cutters have been developed for pre-processing of cylindrical gears for grinding, in which a circle (Fig. 1) which passing through the lower boundary points of involutes B and B1 is used as a palloid of machine gearing of the tool and part. In this case, the active sections of the BE and B1E1 engagement lines are located symmetrically with respect to the axial perpendicular and at some distance from it [1, 4, 5, 6].

The angle of the teeth profile of a special cutter α_K depends on the number of teeth of the machined wheel Z_k and is determined by:

$$\alpha_к = \alpha_B - \sigma_B, \quad (1)$$

Where α_B – is the pressure angle at the lowest point B of the involute; σ_B - is the half of the angle thickness of the tooth at the lower boundary points B and B 1 of the involute.

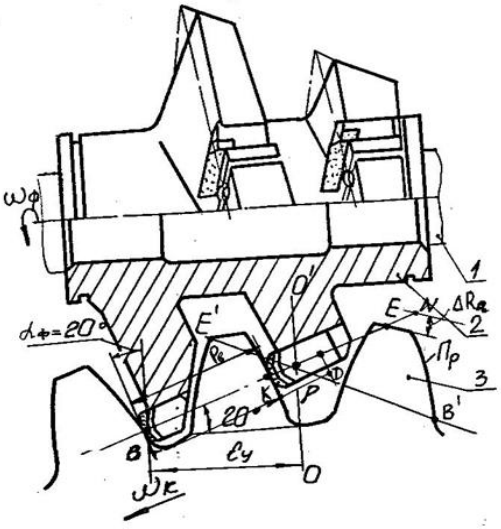

Figure 1 – Scheme of machine engagement of a special carbide cutter with a machined wheel

In the range of cut gear teeth $Z_к = 20…400$, the profile angle of the teeth of special cutters varies within the range of $\alpha_K=5^0\text{-}19^0$

Each mill can cut the teeth of the wheel in a certain range of teeth numbers: $Zк = 33\text{-}49$, $Zк = 46…66$, $Zк = 60…88$, $Zк = 88…134$, $Zк = 134…204$

Technological installation of cutters is achieved by turning one cutter body relative to the other at a certain calculated angle and changing the thickness of the distance ring placed between the bodies. Several keyways are made in each of the cutter bodies.

Figure 2 shows the dependence of the profile angle of the teeth of a special cutter α_k on the number of teeth of the machined wheels Z_K and the displacement coefficient of the original contour of the gear rack X, as well as the range of teeth to be cut [3, 7, 9, 11].

The area of application of the cutters is illustrated in Figure 3. Uncorrected gearwheels with 33 ... 49 teeth could be cut with a milling cutter with a profile angle $\alpha_K = 9^0$ and setting the cutter bodies with a turn at an angle θ

$$\theta = 2z_K\beta_K,$$

where Z_K – is the number of teeth of the cut wheel;

$$\beta_K = \alpha_K - \alpha'_K,$$

where α'_K – is determined from the graph (Fig. 2)

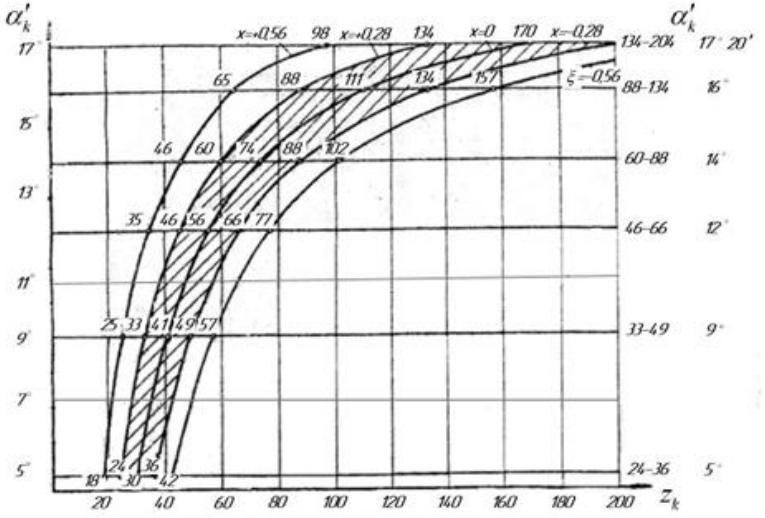

Figure 2 – A Graph for determining the applicability of special carbide milling cutters

For corrected wheels, the range of numbers of teeth to be cut increases: at X = +0,56, using a cutter with $\alpha_K = 9^0$, gear wheels with 25 teeth are cut, and at X = –0,56, gear wheels with 57 teeth are cut

Technological installation of cutters is achieved by turning one cutter hulls relative to the other by a certain design angle (Fig. 3) and changing the thickness of the distance ring Δ, inserted between the cutters hulls. In each of the cutter hulls, several keyways are made [8, 10, 13, 15, 22].

Mills with a given angle α_κ can be used for cutting wheels with a different number of teeth, if the axis of the tooth of the wheel deviates from the axis of the machine (Fig. 3) at an angle β_κ and S_ϕ - the distance between the bodies is recalculated. With positive β_κ, the right cutter body turns clockwise relative to the left one by the angle θ. With negative β_κ - the right cutter body turns counterclockwise and in this position both bodies are fixed to the mandrel.

The rotation of the cutter bodies by an angle θ is carried out by aligning the corresponding keyways in the bodies.

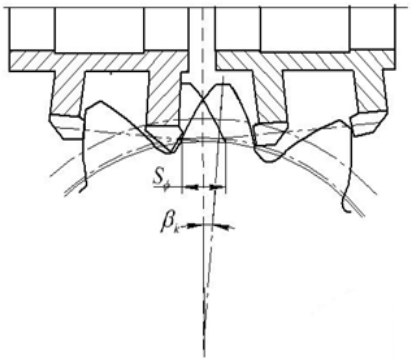

Figure 3 – Installing and adjusting the cutter when turning the wheel at an angle $\beta\kappa$

While being installed on the machine, the bodies of the cutters, which are on the mandrel, are aligned with the first teeth in one plane and set at a distance S_ϕ determined by the conical template (Figure 3, a). The inner distance between the ends of both cutter bodies is measured and a distance ring is selected from it. Then the cutter bodies are installed on the corresponding keyways and fixed on the mandrel. A milling cutter with a mandrel is installed in the machine support with subsequent adjustment relative to the axis of the wheel tooth.

The advantage of the considered design of special hob cutters considered is that both bodies simultaneously treat both lateral surfaces of the wheel teeth. The cutting forces from both bodies are directed towards each other, i.e. there is a force closure inside the tool. This helps to reduce vibrations and oscillations of the machine table together with the processed wheel.

The most rational area of using the considered special mills is the serial and large-scale production of gear wheels, for example, used in coal and ore mills, excavators, rolling mills, lifting mechanisms [1, 12, 14, 17, 20, 21].

Figure 4 shows a special hob cutter m =12 mm. The cutter consists of 2 bodies, separated by a distal ring with tapered threads of one direction.

The development and modeling of the technological process of shaping using universal m = 16 mm single-sided and double-sided cutting mills (Fig. 4) equipped with alloy plates BK10-OM; BK10-XOM. Single-sided cutters (Fig. 4) consist of two bodies: left and right with conical screw threading of turns of the same direction. On the lateral surfaces of the turns in the tangential grooves, hard-alloy non-overlapping rotary plates made of alloys are installed BK10-OM; BK10- XOM with dimensions 20x16x6 mm, which are fixed in the sockets with eccentric screws.

Carbide cutting elements are placed only along the lines of machine engagement of the tool and the workpiece, which makes such a milling cutter more economical in comparison with known designs of similar tools.

The fundamental difference between cutters in comparison with well-known foreign designs (coarse-modular cutters of the company "Azumi", Japan, the company "Fete", [15, 16, 18, 19]) is that with an increased in 1.5-2 times the amount of its teeth over the length of one cutting turn, the above dimensions of the cutting carbide plates are the same for the entire used range of modules m = 16 mm and this, for the first time, a constructive solution reduces the consumption of hard alloy in the manufacture of the tool by 2-5 times, but most importantly, the cutting process is significantly improved with increasing the durability of cutting inserts.

The tangential arrangement of carbide cutting inserts with wear-resistant coatings also contributes to the increase in tool life.

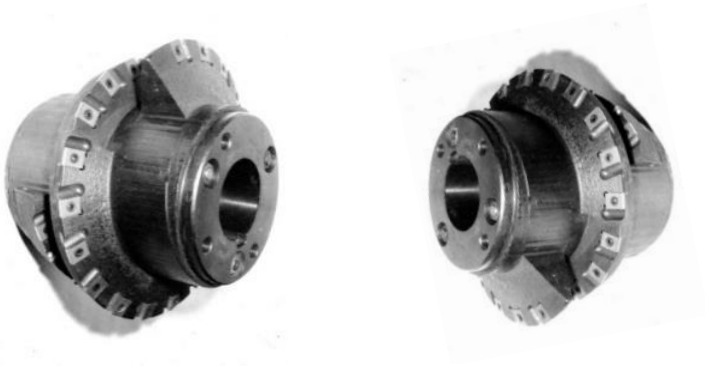

Figure 4 – Special worm-and-carbide double-body cutter
m=16 mm, (a_u=9^0; $Z_к$=19…57)

The technological disadvantage of special carbide milling cutters is the impossibility of processing gear wheels with the same tool, which differ significantly from each other in the number of teeth [15]. Meanwhile, in the practice of heavy engineering, gears are widely used, including a small-toothed gear, for exampl, $z_к$=12÷40 and a multi-toothed wheel, for example $z_к$=180÷316. These are gear drives of coal and ore grinding mills, excavators, etc.

When processing such wheels with different worm cutters, the identity of the main pitch and the profile of the teeth will not be ensured, which will undoubtedly affect the quality of the engagement and the durability of the gear transmission. Of particular importance for the quality of the engagement is the machining of a

mating pair of hardened (HRC56…62) gearwheels with the same tool, the operational running-in of which is practically excluded.

In order to improve the accuracy of engagement of mating, predominantly hardened, gears with a different number of teeth, and to reduce the range of tools used, the design of universal coarse-modular solid carbide hob mills m=10-65 mm has been developed. The pitch circle of the wheel is used as the palloid of the machine gearing of such cutters with the machined wheel, and the profile angle of the tool teeth is equal to $\alpha_и = 20^0$.

The two-body design of single-sided cutters is designed to process wheel teeth in two passes. The milling cutter (Fig. 5) consists of a left 1 and right 2 bodies with a conical screw thread in one direction, in the grooves of which are installed hard-alloy non-overlapping rotary plates.

According to the gear processing technology developed for this design [1, 2], each of the cutter bodies is installed separately on the gear hobbing mandrel with an offset relative to the center perpendicular $00'$ tool-part pair by a distance l_y (Fig. 5, a, b), determined point B (B') of intersection of the circle of the lower boundary point of the involute of the teeth and the line of machine gearing BE ($B' E'$). The setting distance does not depend on the number of teeth of the wheel being machined. The value l_y (Figure 5) is determined by the profiled angle of the initial contour of the rack α 0, the tooth base height h_f and the radius of curvature of the tool head for the preliminary tooth cutting $r_Ф$. These parameters only depend on the modulus and the offset ratio of the original toothed rack contour.

The installation distance is determined by the formula:

$$l_y = \frac{h_f - xm - r_Ф(1 - sin\alpha_0)}{tg\alpha_0}, \quad (2)$$

where x – is the coefficient of displacement of the original contour of the gear rack; m is the module of the teeth of the wheel.

For the wheels with toothed rack source circuit in accordance with GOST 13755-81, where $\alpha_o = 20^0$, h=1,25·m and $r_Ф$. =0,3·m, the formula (2.10) is simplified:

$$l_y = \frac{m*(1.052 - x)}{0.36397}. \quad (3)$$

Thus, by alternately installing each of the bodies with an offset on the gear-cutting mandrel, one cutter can process gears with any number of teeth in two passes. The displacement of the cutter body from the center perpendicular to the calculated distance l_y is carried out by using a special template installed in the machine center finder, which is located on the milling head in the axis of rotation of the machine table.

For convenience of practical definition, Figure 6 shows a graph of the dependence of the installation distance l_y on the modulus of the cut teeth of the wheel and the displacement coefficient of the original contour of the gear rack - x. With the values of the displacement coefficient of the original contour x>1.0, the value of the installation distance l_y, calculated according to (2) and (3), may turn out to be negative. It means that the tool must be moved on the machine during installation, so that, the very first tooth with the largest radius of rotation would not intersect the center perpendicular when displaced.

In practice, setting the tool to the calculated distance l_y does not require high accuracy and can be performed either by using a special template or by using a ruler mounted on the machine support.

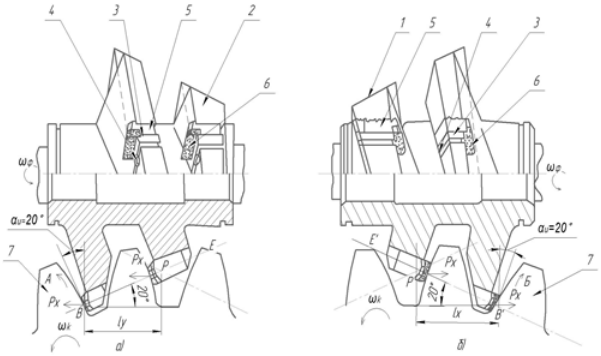

Figure 5 – Two-body, one-sided universal cutter:
а – is the right body; *б* – is the left body
(1 – a tapered thread of the left body; 2 – a tapered thread of the right body;
3 – a pressure plate; 4 – a split slot; 5 – a cutting plate; 6 – an adjustable pin)

The analysis of cutting patterns and kinematics of gear processing with universal double-body cutters [1, 5, 9] shows that when the right-hand housing is in operation (Fig. 5, a), the axial cutting forces P_x coincide with the direction of rotation of the machined wheel ωк (with the direction of rotation of the indexing worm wheel of the machine), and the stock removal proceeds sequentially from the base of the tooth to the top of the same tooth (arrow B).

If the directions of action P_x and ωк coincide, the axial force tends to "separate" the teeth of the pitch worm wheel from the turns of the pitch worm, and this can lead to the disruption in the smooth operation of the pitch worm pair of the machine, vibrations of the processed wheel and decrease in the quality of the processing.

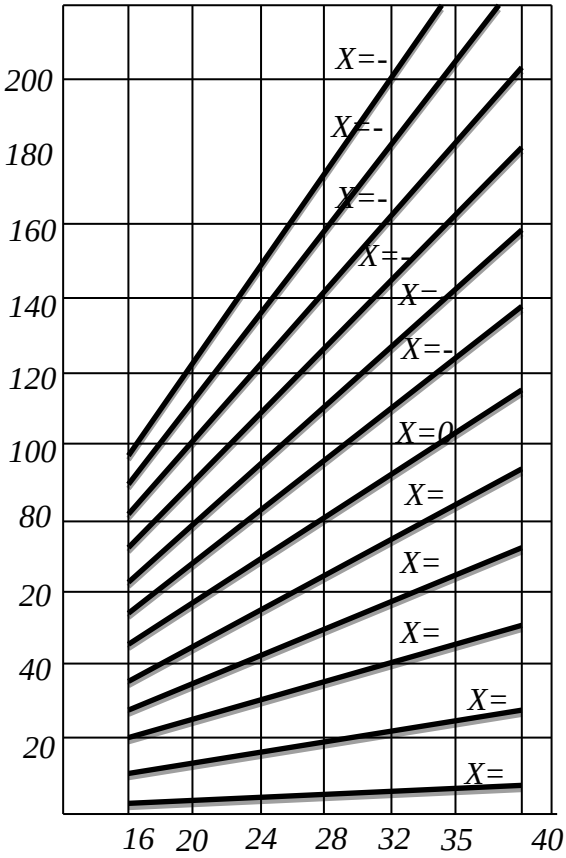

Figure 6 – Graph for determining the installation distance l_y

While removing the allowance in the direction of arrow B (Fig. 5, b), the width of the layers (cut by the teeth of the left housing) is still 2 - 2.5 times greater than that of the teeth of the right housing [1, 4, 7, 9], even it does not exceed the nominal length of the cutting edge of 20 mm.

4. RESULTS AND DISCUSSION

In order to ensure the same processing conditions in terms of cutting dynamics and according to the stock cutting pattern, the cutter bodies can be made with screw threads in different directions. For example: the left-hand cutter body

(Fig. 7) has a right-hand screw thread, and the right-hand cutter body has a left-hand thread. In this case, during machining, the axial components of the cutting force are directed towards the rotation of the wheel $\omega_к$, and the stock removal, carried out by both bodies, goes in the same direction along arrow A - from the base of the tooth to the apex.

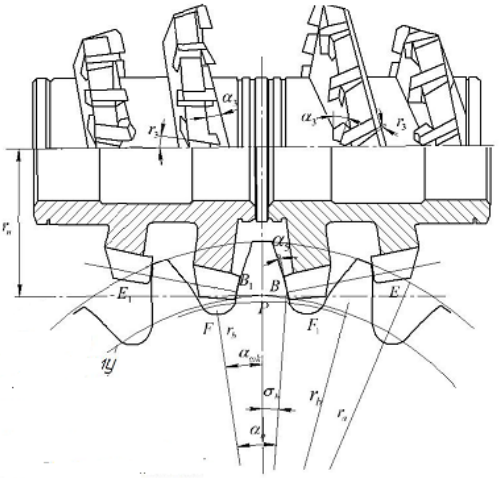

Figure 7 – A scheme of machining the wheel with cutter bodies with different directions of turns

In order to increase the efficiency of using the tool, the processing of both lateral surfaces of the teeth of the wheel could be carried out with only one (either right or left cutter hull), for example, the right cutter body, alternately shifting it to the left and right on the gear-cutting mandrel. In this case (Fig. 8), while processing the left side surfaces, it is necessary to reverse the direction of rotation of the tool $\omega_ф$ and the wheel $\omega_к$ and this processing would be carried out with the accompanying milling [2, 10, 14, 15, 21].

Figure 9 shows a preliminary gear grinding blade processing of the hardened gear wheel m=16 mm; z_k=20; b=155 mm, steel 20X2H4A-III, HRC≥55 in the production conditions at the gear shop of the factory "Svet Shahtyora". The gear hobbing process is carried out with a carbide-tipped hob cutters (Fig. 10) without using the lubricating liquids. The direction of milling is reversed. The cutting conditions for processing hardened teeth are: the depth of the cut t=0.5-0.8 mm per passage; the cutter feed S=1.5-3 mm/rev; the cutter speed: n=40-60 min^{-1}; the cutting speed V=1.0-1.2 m/s.

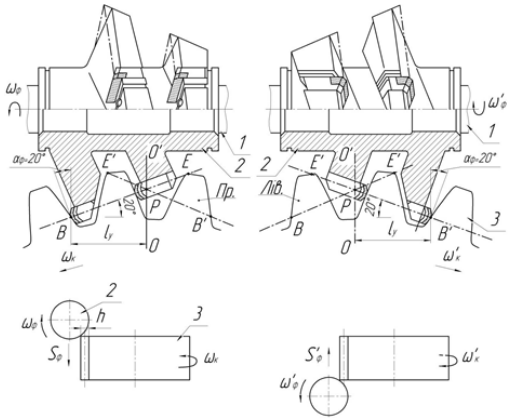

Figure 8 – A scheme of processing wheel teeth with one right-hand cutter body: *а, с* –is a right - hand body during counter milling; *б, d* – is the right body during passing milling with a reversible direction of rotation of the cutter and the gear which is being cut

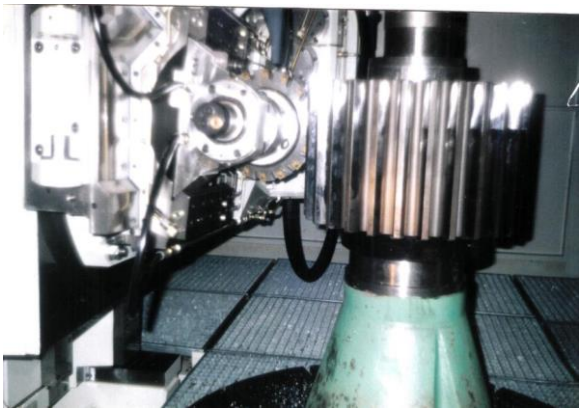

Figure 9 – The pre-treatment with a gear blade for a hardened gear wheel *m=16mm; z=20; β = 0°; b=155 mm*; steel 20Х2Н4А-ІІІ, HRC56…62 at the gear shop of the factory "Svet Shahtyora"

The time of the machine to remove the preliminary allowance for the gear grinding is 35 min. The maximum wear out of the individual cutter teeth, after the specified continuous running time, did not exceed 0.15 mm.

SUMMARY

The use of the developed technological methods of preliminary blade processing of the teeth of hardened wheels with carbide milling cutters makes it possible to reduce the labor intensity of low-performance gear grinding operations, depending on the wheel module, by 3-4 times due to the removal of the main allowance for gear grinding by the method of high-speed gear milling with a special blade tool, in which the allowance is removed according to the line of engagement and does not require the manufacture of the cutting part of the cutter along the height of the entire tooth.

The peculiarity of the design of special hob cutters is that a circle passing through the lower boundary points of the involute is used as the palloid of the machine gearing of the tool and part.

Carbide cutting elements are placed only along the lines of machine engagement of the tool and the workpiece, which makes such a milling cutter more economical in comparison with known designs of similar tools. In order to improve the accuracy of engagement of mating gears with a different number of teeth, and to reduce the range of tools used, the design of universal large-module solid carbide hob cutters m = 16mm has been developed.

A certain cutting section of the cutter tooth is involved in cutting, which ensures economical use of cutting inserts, simplifies the design of cutters, and increases the reliability of the cutting process of hardened cylindrical gears.

References: **1.** O patriarhe zuboobrabotki A.K. Sidorenko / *V.F. Shapovalov, V.I. Pechenyiy, A.A. Klochko, A.N. Korotun, G.I. Mihaylov* // Visnik Natsionalnogo tehnichnogo universitetu "KhPI": zb. nauk. pr. Tematichniy vipusk : Problemi mehanichnogo privodu. – Kharkiv : NTU "KhPI", 2009. – № 20. – pp. 3–7. **2.** *Timofeev Yu. V.* Tehnologiya zubofrezerovaniya zakalennyih krupnomodulnyih koles spetsialnyimi chervyachnyimi frezami s minimiziruyuschimi parametrami glavnyih rezhuschih kromok / Yu. V. Timofeev, A. A. Klochko, V. F. Shapovalov// Naukovi notatki : mizhvuz. zb. – Lutsk, 2010. – Vip. 29. – pp. 209–216. **3.** *Timofeev Yu. V.* Novaya tehnologiya skorostnoy obrabotki zakalennyih krupnomodulnyih zubchatyih koles spetsialnyimi diskovyimi frezami / Yu.V. Timofeev, A.A. Klochko, V.F. Shapovalov// Visnik SevNTU : zb. nauk. pr. Seriya «Mashinopriladobuduvannya ta transport». – Sevastopol, 2011. – Vip. 118. – pp. 139–144. **4.** Sovershenstvovanie tehnologii zubonarezaniya chervyachnyimi modulnyimi frezami s kontaktno-reaktivnoy paykoy rezhuschih plastin / E.V. Mironenko, A.A. Klochko, V.F. Shapovalov, V.A. Chmyir // Nadezhnost instrumenta i optimizatsiya tehnologicheskih sistem : sb. nauch. tr. – Kramatorsk : DGMA, 2013. – Vyip. 33. – pp. 3–7. **5.** Konstruktorsko-tehnologicheskie sposobi povyisheniya proizvoditelnosti i kachestva zuboobrabotki krupnogabaritnyih zubchatyih ventsov / E.V. Mironenko, V.F. Shapovalov, A.A. Klochko, S.Yu. Palashek, E.V. Ostapovich // Visnik NTU "KhPI". Seriya: Tehnologiyi v mashinobuduvanni. – Kharkiv : NTU "KhPI", 2015. – № 4 (1113). – pp. 28–32. **6.** *Suslov, A.G.* Tehnologicheskoe obespechenie i povyishenie ekspluatatsionnyih svoystv detaley i ih soedineniy // A. G. Suslov [i dr.] ; pod obsch. red. A. G. Suslova. – Moscow: Izdatelstvo "Mashinostroenie", 2006. – 447 p. (Ser.: Biblioteka Tehnologa). **7.** *Suslov A.G.* Naznachenie, oboznachenie i kontrol parametrov sherohovatosti poverhnostey detaley mashin/ A.G. Suslov; Pod red. I.M. Korsakovoy. – Moscow: Izdatelstvo MGIU, 2010. – 111 p. **8.** Osnovi formoutvorennya poverhon pri mehanIchnIy obrobtsI / N.S.

Ravskaya, O.A. OhrImenko, P.P .Melnichuk, O.V., T.P. NIkolaenko // Navchalniy posibnik z grifom MON Ukrayini (list № 1/11-5203 vid 12.03.2013), Kyiv: Vid. SKD-Druk 2013. **9.** Joseph Stokes, The Theory and Application of the HVOF Thermal Spray Process, 2008, Dublin City University, 206 p., pp. 1 - 14. **10.** Skorostnoe zubofrezerovanie zakalennyih zubchatyih koles / V.F. Shapovalov, A.A. Permyakov, A.A. Klochko, A.N. Lishenko // Vazhke mashinobuduvannya. Problemi ta perspektivi rozvitku: materiali pyatnadtsyatoYi Mizhnar. nauk.-tehn. konf., 30 travnya – 1 chervnya 2017 r. / Pid zag. red. V. D. Kovalova. – Kramatorsk : DDMA, 2017. – 96 p. **11.** *Sudhansu Ranjan Das, Amaresh Kumar, Debabrata Dhupal*, 2013, Effect of Machining Parameters on Surface Roughness in Machining of Hardened AISI 4340 Steel Using Coated Carbide Inserts, International Journal of Innovation and Applied Studies, Vol. 2, No. 4, Apr. 2013, pp. 445-453. **12.** *Kane M.M.* Upravlenie kachestvom produktsii mashinostroeniya / M. M. Kane, A. G. Suslov, O. A. Gorlenko i dr.pod obsch. red. d.t.n. M. M. Kane. – Moscow : Mashinostroenie, 2010. – 416 p. **13.** Nanotehnologiya mehanicheskoy obrabotki detaley mashin / Yu. F. Nazarov, A. V. Ivanayskiy, D. S. Sviridenko [i dr.] //Tehnologiya mashinostroeniya.– 2009. – № 6. – pp. 45 – 49. **14.** *Johny Shaida Shaik, K.Rajasekhara Babu*, 2012, Prediction of surface roughness in hard turning by using fuzzy logic, International Journal of Emerging trends in Engineering and Development, Issue 2, Vol.5 (July 2012), pp. 38–49. **15.** Tehnologicheskie vozmozhnosti zuboobrabotki vyisokotochnyih krupnogabaritnyih zubchatyih ventsov / A.N. Shelkovoy, A.A. Permyakov, A.A. Klochko, O.A. Antsyiferova, V.F. Shapovalov // Kompleksne zabezpechennya yakosti tehnologichnih protsesiv ta sistem (KZYaTPS – 2017) : materiali tez dopovidey VII mizhnarodnoyi naukovo-praktichnoyi konferentsiyi (m. Chernigiv , 24–27 kvit. 2017 r.) : u 2-h t. / Chernigivskiy natsionalniy tehnologichniy universitet [ta in.]; vidp. za vip.: Eroshenko Andriy Mihaylovich [ta in.]. – Chernigiv : ChNTU, 2017. – T. 1. – pp. 163– 164. **16.** Pat. 2064376 Rossiyskaya Federatsiya,MKI V23 F 5/08, 5/12. Zuboobrabatyivayuschiy stanok / V.F. Shapovalov, V.I. Pechenyiy, A.A. Klochko, S.P. Naletov, N.I. Aristarhov, V.D. Korotkov, G.N. Ruin., N.A. Lobanov, A.V. Kuznetsov. – # 4915857 ; zayavl. 23.01.91 ; opubl. 27.07.96, Byul. # 21. – 5 p. **17.** *Yamnikov, A. S.* Resursosberegayuschie tehnologii izgotovleniya tsilindricheskih zubchatyih koles / A.S. Yamnikov, A.A. Malikov, E.N. Valikov, A.V. Sidorkin // Tehnologiya mashinostroeniya.– 2008. – № 7.– pp. 7–10. **18.** Pat. 2082567 Rossiyskaya Federatsiya,MKI V23 F 5/00. Zuboobrabatyivayuschiy stanok /V. F. Shapovalov, V. I. Pechenyiy, A. A. Klochko, G. N. Ruin, S. P. Naletov, N. I. Aristarhov, V. D. Korotkov, N. A. Lobanov, A. V. Kuznetsov. – № 92009350 ; zayavl. 01.12.92 ; opubl. 27.06.97, Byul. № 18. – 6 p. **19.** Tehnologiya remonta i vosstanovleniya krupnomodulnyih zakalennyih zubchatyih koles metodom vyisokoskorostnoy lezviynoy obrabotki / A.A. Klochko, A.N.Shelkovoy, V.F. Shapovalov, A.V. Belovol, O.A. Antsyiferova // Suchasniy stan naukovih doslidzhen ta tehnologiy v promislovosti. – Kharkiv. 2017. – № 2 (2). – pp. 38–47. **20.** *Shapovalov V.F., Pechenyiy V.I., Klochko A.A., Permyakov A.A., Shelkovoy A.N., Gasanov M.I., Antsyiferova O.A.* Povyishenie kachestva poverhnostnogo sloya zubyev iznoshennyih i vosstanavlivaemyih krupnogabaritnyih zubchatyih koles poverhnostnyim plasticheskim deformirovaniem // Nadiynist Instrumentu ta optimizatsiya tehnologichnih sistem: zb.nauk. pr. – Kramatorsk : DDMA, 2018. – Vip. 42. – pp. 91–102. **21.** *Kovalev V.D., Klimenko S.A., Antonyuk V.S., Vasilchenko Ya.V., Klochko A.A., Ryabchenko S.V., Voloshin O.I. ,Statkevich O.V., Ivanov S.O.* Stvorennya ta vprovadzhennya Innovatsiynih tehnologiy vigotovlennya krupnogabaritnih reduktoriv vazhkogo mashinobuduvannya. Vazhke mashinobuduvannya. Problemi ta perspektivi rozvitku. Materiali Mizhnarodnoyi naukovo-tehnichnoyi konferentsiyi 04 – 07 lipnya 2019 roku / Pid zag. red. V. D. Kovaleva. – Kramatorsk: DDMA, 2019. – pp. 5–6. **22.** *Permyakov O.A., Klochko O.O., Kamchatna-Stepanova K.V., Novikov F.V.* Cherv'yachna freza z rozdilnoyu shemoyu formoutvorennya z povorotnimi neperetochuvanimi rIzalnimi elementami. Novyie i netraditsionnyie tehnologii v resurso- i energosberezhenii: Materialyi mezhdunarodnoy nauchno-tehnicheskoy konferentsii, 22–24 sentyabrya 2021 g., g. Odessa. – Odessa: Gosudarstvennyiy universitet «Odesskaya politehnika», 2021. – pp. 133 – 134.

ОБРОБКА ЗАГАРТОВАНИХ ЦИЛІНДРИЧНИХ ЗУБЧАСТИХ КОЛІС РЕДУКТОРА РІЗАННЯ КОМБАЙНА УКД 200-500

Анотація. *У статті розглянуті останні розробки унікальних технологічних прийомів зубофрезерування циліндричних зубчастих коліс для попередньої лезової зубообробки загартованих циліндричних зубчастих коліс редуктора різання вугледобувного комбайна УКД200-500 для остаточного зубошліфування зубів зубчастих коліс з модулем 16. Для швидкісної лезової зубообробки розроблено, виготовлено та впроваджено в виробництво перспективні конструкції черв'ячних твердосплавних фрез. Для експлуатації кожного з конструктивних рішень твердосплавних черв'ячних фрез розроблені технологічні регламенти лезової зубообробки. Розроблено конструкцію спеціальної двокорпусної черв'ячної фрези двостороннього різання. Особливість проектування спеціальних черв'ячних фрез полягає в тому, що як палоїда верстатного зачеплення інструменту і деталі використовується коло, що проходить через нижні граничні точки евольвенти. Твердосплавні різальні елементи розміщені тільки по лініях верстатного зачеплення інструменту та заготовки, що робить таку фрезу економічнішою порівняно з відомими конструкціями аналогічних інструментів. З метою підвищення точності зачеплення сполучних, зубчастих коліс з різним числом зубів, і скорочення номенклатури інструменту розроблена конструкція універсальних великомодульних твердосплавних черв'ячних фрез m=16мм. Застосування розроблених технологічних прийомів попередньої лезової обробки зубів загартованих коліс твердосплавними фрезами дозволяє знизити трудомісткість малопродуктивних зубошліфувальних операцій, залежно від модуля коліс, у 3-4 рази за рахунок зменшення припуску з 1,5-2,5 мм на бік зуба до 0,3 -0,5 мм, а також дозволяє забезпечити економічність процесу зубообробки за рахунок зменшення витрат твердосплавних пластин.*

Ключові слова: *технологічні прийоми; крупномодульні циліндричні загартовані зубчасті колеса; швидкісна лезова зубообробка.*

UDC 622.23.05+621.83 **doi: 10.20998/2078-7405.2021.95.08**

O. Koval'chuk, R. Berezhnyj, V. Nezhebovs'kyj,
O. Ustynenko, Kharkiv, Ukraine

ANALYSIS OF TENSENESS AND DURABILITY OF THE MAIN PARTS FOR THE CUTTING PART OF UKD 200-500 COAL SHEARER

Abstract. *JSC "Kharkiv Machine-Building Plant "Svitlo Shahtarja" has created and introduced into serial production a new generation UKD200-500 coal shearer. The most loaded element of the shearer is its cutting part. It is a three-stage reducer with an electric motor. Calculations for the strength and durability of gearing, shafts, bearings, spline, pinned and hinge joints have been carried out. The modeling of the stress-strain state for the main parts and assemblies by the finite element method has also been carried out. Calculations have shown that the strength and durability of all parts is ensured. Consequently, the required durability of 15000 hours and the average resource before major overhaul are not less than 800...1000 thousand tons are provided.*
Keywords: *coal shearer; cutting part; gear; strength; durability; stress.*

1. INTRODUCTION

The current state of the Ukrainian fuel and energy complex requires a continuous increase in coal production. Currently, 80% of coal deposits are in thin seams.

As part of the implementation of the concept of development of the coal industry, approved by the order of the Cabinet of Ministers of Ukraine No. 236-r dated July 7, 2005 [1], in order to extract coal from thin seams, JSC "Kharkiv Machine-Building Plant "Svitlo Shahtarja" created and introduced into serial production a new generation UKD200-500 coal shearer. It is designed for mechanized coal extraction as part of mining complexes, in longwalls of shallow and inclined seams 0,85–1,5 m thickness, moving along strike with inclination angles up to 35°, as well as rise and fall with angles up to 10°, with coal cutting resistance up to 480 kN/m. Its technical characteristics are at the level of modern foreign counterparts.

UKD200-500 coal shearer is a cutting action machine equipped with auger executive bodies for destruction and loading of coal onto a conveyor – Figure 1 Moving the shearer with a scraper conveyor is carried out by means of an external feed system.

The most important and loaded element of the shearer is its cutting part – Figure 2, 3. It is a three-stage spur reducer with an electric motor:

– 1st stage is three in-line cylindrical gears, module m = 6 mm;

– 2nd stage is planetary single-stage with fixed epicycle, module m = 6 mm;

– 3rd stage is four in-line cylindrical gears, module m = 16 mm.

– Darnel K4-16-233 electric motor, rated power 250 kW, rated speed 1470 rpm, asynchronous three-phase with squirrel-cage rotor.

Figure 1 – The UKD200-500 coal shearer

The cutting part of the UKD200-500 coal shearer is unified. This allows it to be installed on either the left or right side of the frame. Each reducer stage is located in a separate sealed chamber, protected from the penetration of abrasive particles.

The material of external gears is Steel 20Ch2N4ASh, with heat treatment – carburizing followed by quenching and low tempering. Material of the planetary stage epicycle – Steel 40 ChN, with heat treatment – improvement for hardness 270–300HB.

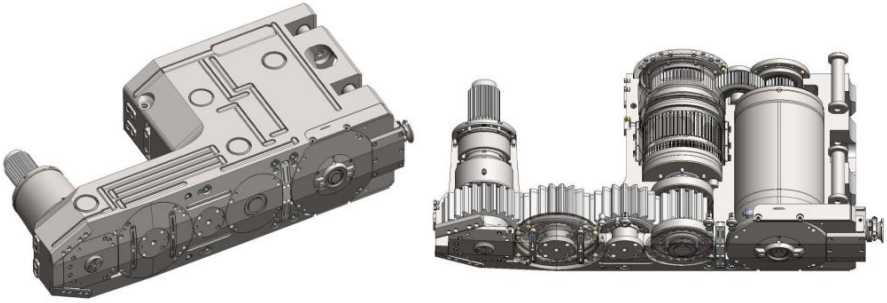

Figure 2 – The cutting part of UKD200-500 coal shearer

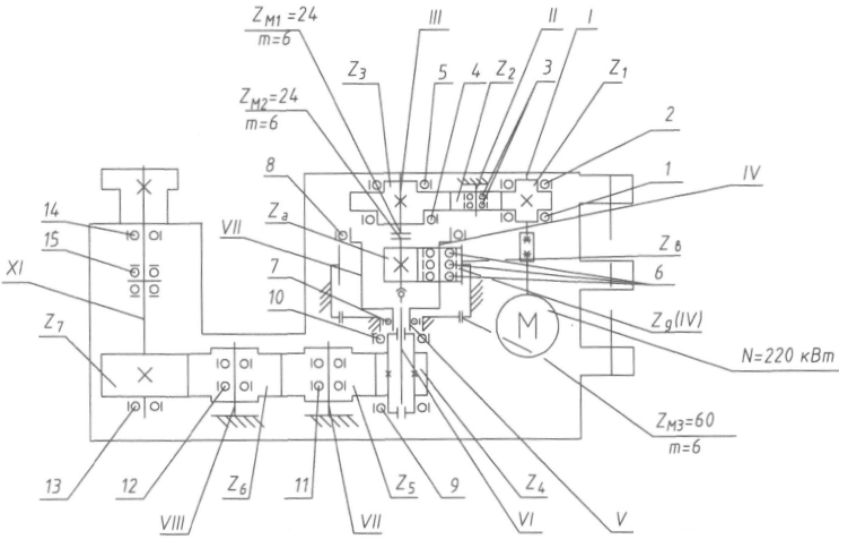

Figure 3 – Kinematic diagram of the cutting part reducer

2. PROBLEM STATEMENT

Reliability and durability of the shearer as a whole depend on the reliability and durability of the cutting part, mainly its gears. It is necessary to take into account that coal mining equipment operates in especially difficult conditions. These are elevated temperatures, a wide range of shock loads and extremely high dust levels. In this case, it is required to ensure the high durability of gears and bearings – at least 15000 hours. Based on this, during the design process, as well as in the future, taking into account the operating experience, a large amount of calculations of its main parts for strength and durability was performed, namely:

– calculations for contact and bending fatigue and static strength of gearings;
– calculations of shafts for static and fatigue strength;
– calculation of service life and static strength of bearings;
– calculations of spline, pinned and hinge joints;
– modeling of the stress-strain state for the main parts and assemblies by the finite element method.

Next we will consider the methods, approaches and results of the performed calculations. For gears, as the main and most critical drive element, they will be presented in more detail. For the rest of the calculations, due to the limited volume of the article, we will present only the main results.

3. MATERIALS AND METHODS

Let's start with *the basic initial data*.

The design load was taken as follows:

– rated torque T_r = 1624 N·m;

– the maximum long-term operating torque for calculating the durability T_{rM} = 3090 N·m [2];

– the maximum short-term torque for calculating the static strength T_M = 5740 N·m [3].

The total estimated resource of the combine is 15000 hours. We assume that each of the two cutting parts works for half of the calculated resource with nominal loads. Therefore, the estimated life for the cutting part is 7500 hours.

The calculation of the gearing geometry, contact and bending stresses in them was carried out on the basis of standard techniques [4–7]. Also, the permissible stresses were refined on the basis of mathematical modeling for fatigue processes in the teeth [8].

The assessment of durability was carried out using the recommendations of GOST 21354–87 [6]: the slight slope of the right branch of the contact fatigue curve was taken into account at the total numbers of stress change cycles $N_K > N_{H\lim}$. Here $N_{H\lim}$ is the base numbers of cycles corresponding to the contact fatigue limit $\sigma_{H\lim b}$ – Figure 4.

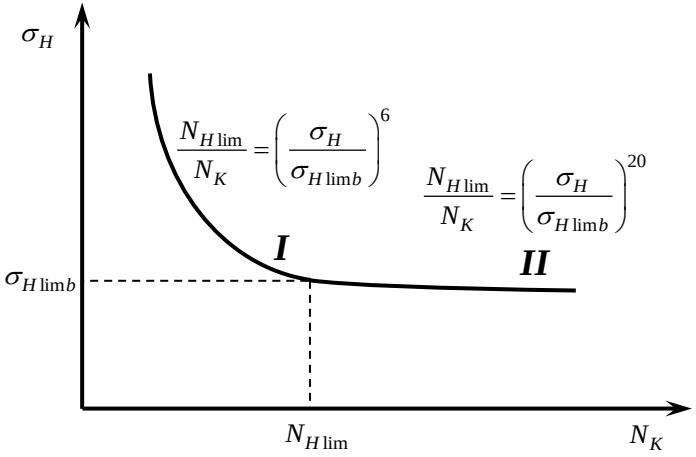

Figure 4 – Contact fatigue curve of active tooth surfaces:
I – zone of limited fatigue; *II* – zone of long-term fatigue

The resource calculation was carried out in the next sequence.

1. The equivalent numbers of stress change cycles were determined for calculating the contact and bending fatigue N_{HE} and N_{FE} according to the next formulas [6]:

$$N_{HE} = \sum_{i=1}^{i_n} \left(\frac{T_{1i}}{T_{1H}} \right)^3 N_{ci}\,; \quad N_{FE} = \sum_{i=1}^{i_n} \left(\frac{T_{1i}}{T_{1F}} \right)^{q_F} N_{ci} \le N_{F\lim}\,, \tag{1}$$

where $i = 1;\ldots; i_n$ – accepted for calculation load steps in the cyclorama; T_{1i} and $N_{ci} = 60 n_i \cdot t_i$ – corresponding values of torque and stress cycles on the pinion; $N_{F\lim}$ – base number of cycles corresponding to the bending fatigue limit $\sigma^0_{F\lim b}$; $q_F = 9$ for the case of surface chemo-heat treatment of teeth and an unpolished tooth root; $q_F = 6$ for other variants of heat treatment or polished tooth root.

Additionally, for case $N_K > N_{H\lim}$, steps with loads that create stresses below the so-called damaging level $\sigma_{HG} = \alpha_{HG} \cdot \sigma_{H\lim b}$ were excluded from the cyclorama. GOST 21354–87 recommends $\alpha_{HG} = 0{,}75$ [6].

2. The total number of cycles to failure was calculated.

2.1. Bending fatigue:

$$\left.\begin{aligned} N_{F\Sigma 1(2)} &= \left(\frac{\sigma_{FP1(2)}}{\sigma_{F1(2)}} \right)^{q_F} N_{FE1(2)} \quad \text{if } N_{F\Sigma 1(2)} \le N_{F\lim 1(2)}; \\ N_{F\Sigma 1(2)} &= \infty \qquad\qquad\qquad\qquad\quad \text{if } N_{F\Sigma 1(2)} > N_{F\lim 1(2)}. \end{aligned}\right\} \tag{2}$$

2.2. Contact fatigue:

$$\left.\begin{aligned} N_{H\Sigma} &= N_{HE} \left(\frac{\sigma_{HP}}{\sigma_H} \right)^6 \quad \text{if } N_{HE} \le N_{H\lim}; \\ N_{H\Sigma} &= N_{HE} \left(\frac{\sigma_{HP}}{\sigma_H} \right)^{20} \quad \text{if } N_{HE} > N_{H\lim}. \end{aligned}\right\} \tag{3}$$

3. The calculated durability of the teeth was determined by contact and bending fatigue in hours, L_{Hh} and L_{Fh}:

$$L_{Hh} = t \frac{N_{H\Sigma}}{N_{HE}}\,; \quad L_{Fh} = \min\left\{ t \frac{N_{F\Sigma 1}}{N_{FE1}}, t \frac{N_{F\Sigma 2}}{N_{FE2}} \right\}, \tag{4}$$

where t – required resource of gears.

The minimum of L_{Hh} and L_{Fh} was taken as the final value of the durability L_h for each gear pair.

Calculations of shafts, bearings, spline, pinned and hinge joints were carried out on the basis of generally accepted engineering techniques, for example [9].

Modeling of the stress-strain state for the main parts and assemblies by the finite element method was carried out in specialized software ANSYS [10] and Autodesk Inventor Nastran (Nastran In-CAD) [11]. The carrier of the planetary stage, reducer housing, shafts, spline parts, etc. were research.

4. RESULTS AND DISCUSSION

Calculation results of strength and durability for gearings of the cutting part reducer are presented in Table 1.

Analysis of the data in Table 1 shows that the strength and durability for all gears of the cutting part are ensured.

Table 1 – Calculation results of gears strength and durability

Gear	1st stage			2nd (planetary) stage			3rd stage			
Number of teeth	Z_1 23	Z_2 43	Z_3 50	Z_a 15	Z_g 23	Z_b 60	Z_4 14	Z_5 20	Z_6 20	Z_7 24
Module *m*, mm	6			6			16			
Contact fatigue safety factor S_H ($[S_H]$ = 1,2)	1,45	1,74	1,90	1,24	1,72	1,42 $[S_H]$=1,1	1,66	1,98	2,19	2,01
Bending fatigue safety factor S_F ($[S_F]$ = 1,55)	2,72	2,12	2,97	2.83	2,45	3,19 $[S_F]$=1,7	2,92	2,78	2,78	3,05
Contact static strength safety factor S_{HM} ($[S_{HM}]$ = 1)	1,93	1,93	2,32	1,71	1,71	1,69	1,50	1,50	1,65	1,65
Bending static strength safety factor S_{FM} ($[S_{FM}]$ = 1,75)	3,62	3,50	3,59	3,79	3,69	4,74	2,89	3,52	3,87	2,77
Calculated service life of teeth *t*, hours	330200	$12{,}7\cdot10^6$	$73{,}5\cdot10^6$	14400	810500	$1{,}2\cdot10^6$	52500	151300	277100	165600

Next are some of the *main calculation results for shafts, bearings and joints.*

For shafts:

– the calculated safety factors of fatigue strength are in the range n = 1,55…15,47 with the minimum allowable value $[n]$ = 1,5;

– the calculated safety factors of static strength are in the range n_M = 1,55…20,33 with the minimum allowable value of yield strength $[n_M]$ = 1,5;

For bearings:

– the calculated service life in terms of dynamic load capacity is in the range L_h = 8000…$4 \cdot 10^7$ h with the required service life [L_h] = 75000 h;

– the calculated safety factors in terms of static load capacity are in the range n_0 = 1,5…26,0 with the minimum allowable value [n_0] = 1,0;

For joints:

– in spline joints, the calculated safety factors of contact stress are in the range n_σ = 2,68…6,17 with the minimum allowable value [n_σ] = 1,0;

– in pinned joints, the calculated safety factors of contact and shear stress are in the range $n_{\sigma(\tau)}$ = 1,68…7,97 with the minimum allowable value [$n_{\sigma(\tau)}$] = 1,0;

– for the axes of the hinge joints, the calculated safety factors of static strength are in the range n_M = 1,21…2,8 with the minimum allowable value [n_M] = 1,2.

Analysis of these results shows that the strength and durability for the main elements of the cutting part are ensured.

In conclusion, we will give an example of *modeling the stress-strain state for main parts and assemblies using the finite element method.* Figure 5 shows the distribution of equivalent von Mises stress, MPa, in auger splined bushing.

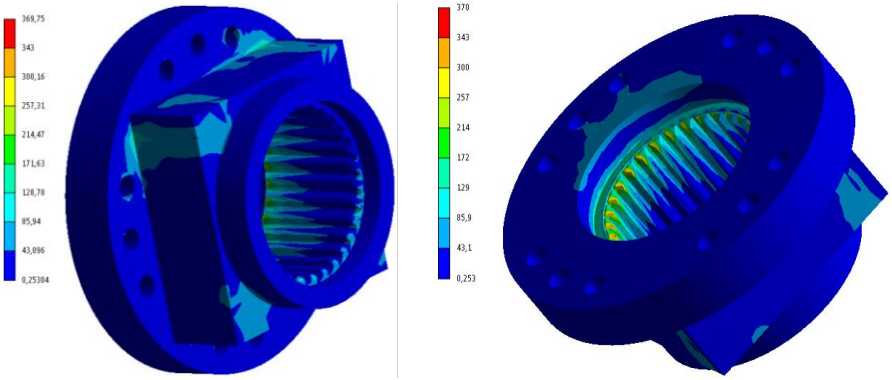

Figure 5 – Equivalent stress by von Mises, MPa, in auger splined bushing

The highest stresses occur in the concentration zone at the edges of the spline teeth. However, in the contact zone of the bushing with the auger, the stress is less than 100 MPa. This satisfies the strength conditions.

SUMMARY

A detailed assessment of the tenseness and durability of the main parts and assemblies for the cutting part of the UKD200-500 new generation shearer has been carried out. It was created and introduced into serial production at the JSC "Kharkiv Machine-Building Plant "Svitlo Shahtarja". In terms of technical characteristics, the shearer corresponds to modern foreign counterparts.

Calculations and modeling of the stress-strain state showed:

– the strength and durability of all gears and shafts are ensured;
– the calculated service life in terms of dynamic load capacity for all bearings are ensured. Safety factors in terms of static load capacity exceed the minimum allowable values;
– the calculated safety factors of strength for spline, pinned and hinge joints exceed the minimum allowable values;
– modeling of the stress-strain state by the finite element method made it possible to evaluate the strength of parts and assemblies of complex configuration. Calculations have shown that, in terms of the level of maximum stresses, all parts correspond the strength conditions.

Thus, it can be concluded that the developed cutting part design of the UKD200-500 coal shearer provides the required durability of 15000 hours and the average resource before overhaul (depending on the resistance of the coal to cutting) not less than 800...1000 thousand tons.

References: 1. Koncepcija rozvytku vugil'noi' promyslovosti. Shvaleno rozporjadzhennjam Kabinetu Ministriv Ukrai'ny vid 7 lypnja 2005 r. No 236-r [The concept of development of the coal industry. Approved by the order of the Cabinet of Ministers of Ukraine of July 7, 2005 No 236-r]. Available at: https://www.kmu.gov.ua/npas/18609693 (accessed 19 December 2021). **2.** KD 12.10.042–99. Izdelija ugol'nogo mashinostroenija. Kombajny ochistnye. Metodika vybora spektrov jekspluatacionnoj nagruzhennosti transmissij [KD 12.10.041–99. Coal engineering products. Coal shearers. Methodology of the spectrum selection for operational loading of transmissions]. Kyiv, 1999. **3.** KD 12.10.042–99. Izdelija ugol'nogo mashinostroenija. Kombajny ochistnye. Metodika rascheta maksimal'nyh nagruzok v transmissijah [KD 12.10.042–99. Coal engineering products. Coal shearers. Methodology for calculating the maximum loads in transmissions.]. Kyiv, 1999. **4.** GOST 16532–70. Peredachi zubchatye cilindricheskie jevol'ventnye vneshnego zaceplenija. Raschet geometrii [State Standard 16532–70. Cilindrical involute external gear pairs. Calculation of geometry]. Moscow, Standarts Publ., 1983. 43 p. **5.** ISO 21771:2007 Gears. Cylindrical involute gears and gear pairs. Concepts and geometry. 2007. **6.** GOST 21354–87. Peredachi zubchatye cilindricheskie jevol'ventnye vneshnego zaceplenija. Raschet na prochnost' [State Standard 21354-87. Cylindrical evolvent gears of external engagment. Strength calculation]. Moscow, Standarts Publ., 1989. 76 p. **7.** ISO 6336:2006 Metod B. Calculation of load capacity of spur and helical gears. 2006. **8.** *Ustinenko A.V.* Matematicheskoe modelirovanie processov ustalostnogo razrushenija zub'ev [Mathematical modeling of processes of fatigue failure teeth]. Visnyk NTU "KhPI". Zbirnyk naukovykh prats'. Serija Mashynoznavstvo ta SAPR [Bulletin of the NTU "KhPI". The collection of scientific works. Series Engineering and CAD], 2012, no. 22, pp. 170–175. **9.** *Pavlyshhe V. T.* Osnovy konstrujuvannja ta rozrahunok detalej mashyn [Fundamentals of design and calculation of machine parts]. L'viv, Afisha Publ., 2003. 560 p. **10.** ANSYS: Engineering Simulation Software. Available at: https://www.ansys.com/ (accessed 19 December 2021). **11.** *Inventor*

Nastran: CAD-embedded finite element analysis. Available at: https://www.autodesk.com/products/inventor-nastran/overview (accessed 19 December 2021).

Олександр Ковальчук, Роман Бережний, Володимир Нежебовський,
Олександр Устиненко, Харків, Україна

АНАЛІЗ НАПРУЖЕНОСТІ ТА ДОВГОВІЧНОСТІ ОСНОВНИХ ДЕТАЛЕЙ РІЖУЧОЇ ЧАСТИНИ ОЧИСНОГО КОМБАЙНУ УКД 200-500

Анотація. *АТ "Харківський машинобудівний завод "Світло шахтаря" створив та впровадив у серійне виробництво очисний комбайн нового покоління УКД 200-500. Найбільш відповідальним та навантаженим елементом комбайна є його ріжуча частина. Вона являє собою триступінчастий прямозубий редуктор з електродвигуном. Ріжуча частина є уніфікованою. Це дозволяє встановлювати її як з лівого, так і з правого боку рами. Кожен ступінь редуктора розташований в окремій герметичній камері, захищеній від проникнення абразивних частинок. У процесі проектування було виконано великий обсяг розрахунків його основних деталей на міцність та довговічність: контактної та згинальної міцності та витривалості зубчастих зачеплень; валів на статичну та втомну міцність; терміну служби та статичної міцності підшипників; шліцьових, штифтових та шарнірних з'єднань; моделювання напружено-деформованого стану основних деталей та вузлів методом скінченних елементів. Розрахунки зубчастих передач, валів, підшипників шліцьових, штифтових та шарнірних з'єднань виконувались за допомогою загальноприйнятих інженерних методик. Також для зубчастих передач уточнювали допустимі напруження на основі математичного моделювання втомних процесів у зубцях. Розрахунки показали, що міцність та довговічність усіх зубчастих коліс та валів забезпечені; розрахунковий термін служби по динамічній вантажопідйомності усіх підшипників забезпечений, а запаси по статичної вантажопідйомності перевищують мінімально допустимі значення; розрахункові запаси міцності для шліцьових, штифтових та шарнірних з'єднань перевищують мінімально допустимі значення. Моделювання напружено-деформованого стану за допомогою метода скінченних елементів дозволило оцінити міцність деталей та вузлів складної конфігурації, таких як корпус, водило планетарного ступеня та інших. Ці розрахунки показали, що за рівнем максимальних напружень усі деталі задовольняють умовам міцності. Це дозволяє зробити висновок, що розроблена конструкція ріжучої частини комбайна забезпечує необхідну довговічність 15000 год та середній ресурс до капітального ремонту (залежно від опірності вугілля різанню) не менше 800…1000 тис. т.*

Ключові слова: *очисний комбайн; ріжуча частина; зубчаста передача; міцність; довговічність; напруження.*

CONTENT

Kovalev V., Klymenko G., Vasylchenko Y., Shapovalov M., Antsiferova O., Maiskykh I. Results of industrial testing of carbide cutting tools by pulsed magnetic field treatment and the effect on the increase of the cutting process efficiency 3

Matyi H., Tamás P. Digital twin technology in logistics literature review 13

Molnár Z., Tamás P., Illés B. Using the slp method in the design of flexible manufacturing cells 22

Nagy A., Kundrák J. Analysis of the change in roughness on a face-milled surface measured every 45° direction to the feed 29

Strelchuk R., Shelkovyi O. Research of the cutting mechanism at electrical discharge grinding 37

Yakimov O., Uminsky S., Klimenko N., Kirkopulo K., Pavlyshko A., Vaysman V. Improving grinding of gear wheels applied in gearboxes of power engineering 45

Koval'chuk O., Nezhebovsky V., Permyakov O., Klochko O., Ryabchenko S. Processing of hardened cylindrical gear wheels of the cutting gearbox of the combine UKD 200-500 57

Koval'chuk O., Berezhnyj R., Nezhebovs'kyj V., Ustynenko O. Analysis of tenseness and durability of the main parts for the cutting part of UKD 200-500 coal shearer 71

Наукове видання

РІЗАННЯ ТА ІНСТРУМЕНТИ
в технологічних системах

Міжнародний науково-технічний збірник

Випуск № 95

Укладач *д.т.н., проф. О.М. Шелковий*
Оригинал-макет *А.М. Борзенко*
Відп. за випуск *к.т.н., проф. Є.В. Островерх*

В авторській редакції

Матеріали відтворено з авторських оригіналів

Підп. до друку 12.02.2019.Формат 60x84 1/16. ПапірСоруРарег.
Друк - ризографія. Гарнитура Таймс. Умов.друк.арк. 10,93. Облік.вид.арк. 11,0. Наклад 300 прим.
1-й завод 1-100. Зам. № 1149. Ціна договірна.

Видавничий центр НТУ «ХПІ»
Свідоцтво про державну реєстрацію ДК № 116 від 10.07.2000 р.
61002, Харків, вул. Кирпичова, 2